# We are IntechOpen, the world's leading publisher of Open Access books
# Built by scientists, for scientists

## 6,900
Open access books available

## 186,000
International authors and editors

## 200M
Downloads

Our authors are among the

## 154
Countries delivered to

## TOP 1%
most cited scientists

## 12.2%
Contributors from top 500 universities

**CLARIVATE ANALYTICS**
**BOOK CITATION INDEX**
**INDEXED**

**WEB OF SCIENCE™**

Selection of our books indexed in the Book Citation Index
in Web of Science™ Core Collection (BKCI)

## Interested in publishing with us?
## Contact book.department@intechopen.com

Numbers displayed above are based on latest data collected.
For more information visit www.intechopen.com

# The Role of Geoelectrical DC Methods in Determining the Subsurface Tectonics Features. Case Studies from Syria

Jamal Asfahani[1]
*Atomic Energy Commission*
*P.O. Box 6091, Damascus,*
*Syria*

## 1. Introduction

The tectonic and faulted zones are characterized by a pronounced change in rock physical properties, where the application of geophysical methods allows directly detecting and delineating such zones. The geoelectrical DC methods are the most appropriate for characterizing the tectonic and faulted zones. Different DC configurations have been developed for the location of tectonic and faulted zones, such as combined resistivity profiling, (Mares *et al.*, 1984).

In the last few years, a large number of high-resolution seismic reflection surveys have been conducted ( e.g., Williams et al.,1995; Palmer et al., 1997; Van Arsdale et al., 1998 to provide information on Quaternary fault geometry and timing. For very shallow investigation, ground-penetrating radar (GPR), which can bridge the gap between high-resolution seismic surveys and trenching, has been applied by Cai et al. (1996) in the San Francisco Bay region. Although, the GPR yields a high- resolution picture down to 4 to 6 m, but the high number of GPR reflections and diffractions resulting from complex sedimentary and tectonic features does not usually permit an unambiguous location of fault, (Demanet et al. (2001). However, when the fault is delineated by other geophysical methods, the interpretation of GPR data gives valuable information on the deformation pattern close to the fault and its position.

At the border of Nevada and California, Shields et al. (1998) have used several geophysical techniques (seismic reflection, magnetic, and electromagnetic) to locate the extension of the Parhump Valley fault zone. Demanet et al. (2001) have also applied various geophysical techniques (electrical profiling, electromagnetic, GPR, seismic reflection) along the Bree fault scrap (Western border of the Roer Graben) in order to locate and image an active fault zone in a depth range between a few decimeters to a few tens of meters. These acquired geophysical data are considered as a reconnaissance tool prior to trenching. Parrales et al., 2003 has executed a site investigation by using combined geophysical methods in a faulted area in Managua, Nicaragua. A mapping of active capable faults by high resolution geophysical methods has been carried out by Chwatel et al., 2005, where several examples from the Central Vienna basin were provided. Caputo et al., 2007, 2003 have characterized

---

[1] jasfahani@aec.org.sy

the late Quaternary activity along the Scorciabuoi fault (Southern Italy) as inferred from electrical resistivity tomographies. Piscitelli et al., 2009 showed tomography examples in studying active tectonics from the Tyrnavos basin, Greece. The characterization of Quaternary faults by electric resistivity tomography in the Andean Precordillera of Western Argentina has also been shown by Sabrina et al., 2009.

More recently, Massoud *et al.*, 2009 have applied the directional azimuthal resistivity sounding and joint inversion of VES-TEM data to delineate the shallow subsurface structure near Lake Qaroun, El Fayoum in Egypt.

Asfahani, 2007 ( a, and b), Asfahani, 2010-a has applied the geoelectrical DC method, particularly VES soundings in the Khanaser valley in Northern Syria to estimate the water resources. He has delineated subsurface structures and outlined fresh, brackish and saline water accumulations through treating the VES data by applying Pichugin Habibulaiev technique (1985). Asfahani in the paper of (Asfahani and Radwan, 2007) enhanced later the proved efficiency of the Pichugin Habibulaiev technique and made it applicable even in pronounced topography and relief areas. Accordingly, shallow and young subsurface structures were delineated and used thereafter as a basis for deducing the tectonic origin of Khanaser Valley. Asfahani in the paper of Asfahani *et al.*, 2010 has successfully applied different geoelectrical methods in Al-Lujj area, Northwestern Syria in order to explain the subsurface tectonic origin of the Kastoon Dam in the Ghab trough depression.

This chapter mainly concentrates on the use of DC methods, particularly the vertical electrical sounding technique (VES), and the interpretation of the VES data by applying the enhanced Pichugin$ Habibuleav approach for determining the subsurface tectonics in different case problems taken from Syria.

## 2. Vertical Electrical Sounding (VES)

Vertical Electrical Resistivity Sounding (VES) is generally used to determine vertical variations in electrical resistivity. In this technique, an electrical current is imposed by a pair of electrodes at a varying spacing expanding symmetrically from a central point, while measuring the surface expression of the resulting potential field with an additional pair of electrodes at appropriate spacing, (Fig.1). For any array of current electrodes A and B and potential electrodes M and N, apparent resistivity ρa is expressed according to Dobrin (1976) by:

$$\rho a = K . \frac{\Delta V}{I} \tag{1}$$

Where

$$K = \frac{2\pi}{\dfrac{1}{AM} - \dfrac{1}{BM} - \dfrac{1}{AN} + \dfrac{1}{BN}} \tag{2}$$

In the equation [1], $I$ is the current introduced into the earth and $\Delta V$ is the potential measured between the potential electrodes. The instrument used in gathering the field data measures directly the resistance $\dfrac{\Delta V}{I}$, and apparent resistivity ρa is subsequently obtained after computing the geometric coefficient (K) for a given position of current and potential electrodes (Dobrin 1976).
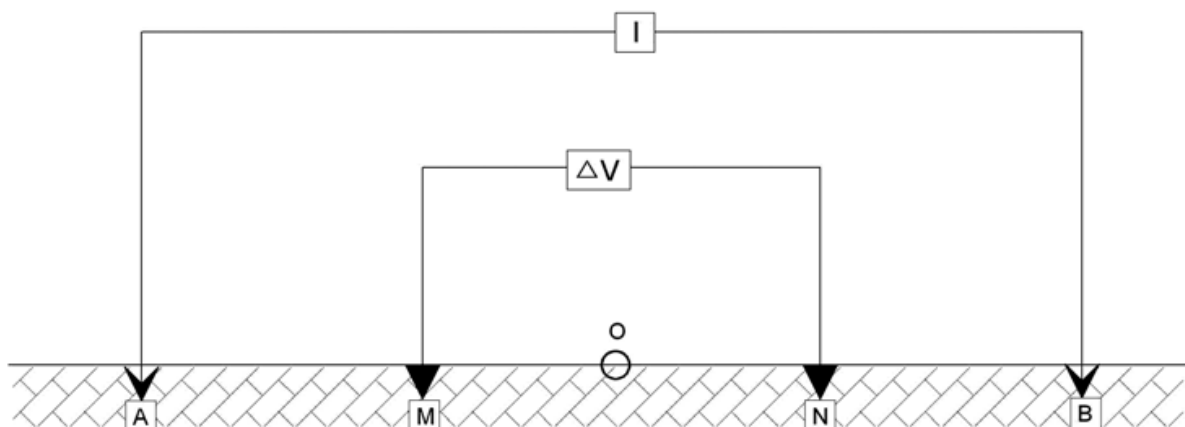
Fig. 1. Schlumberger Configuration in the field.

According to Asfahani; 2010-d a new modification and development on the described traditional Schlumberger configuration consists of using two kinds of AB/2 spacings: The first spacings are purposely designed in order to obtain reliable detailed data on the shallow depths, not exceeding 50m.

The new added AB/2 spacings are:

1, 1.3, 1.68, 2.18, 2.82, 3.66, 4.74, 6.15, 7.97, 10.33, 13.38, 17.35, 22.49, 29.15, 37.78, 48.87, 63.48, 82.27 and 106.6m.

The second traditional AB/2 spacings are:

3,5, 7, 10, 15, 20, 30, 40, 50, 70, 100, 150, 200, 300, 400, 500, 750, 1000, 1500 and 2000m.

In the field application, the two shallow and deep spacings are executed in the same time, such as two-geoelectrical field curves are obtained at a given VES location.

Each of the two obtained field resistivity curves is separately interpreted according to the new proposed interpretation approach consisting of the following three distinguished steps, Asfahani;2010-d:

1. The first interpretation step is achieved by applying the traditional curve matching technique and using the master curves (Orellana and Mooney 1966).
   Accordingly, corresponding subsurface layers thicknesses and resistivities are approximated. The approximate models are thereafter accurately interpreted using an inverse technique program (Zohdy 1989; Zohdy and Bisdorf 1989), until good and reasonable fitness between field and regenerated theoretical curves are obtained.

2. The second interpretation step is achieved by using the technique of PichuginHabibuleav (1985), Asfahani *et al.*, 2007, 2010.
   This interpretative technique is considered as the most sophisticated for distinguishing fractured zones and dipping contacts between different rock types and can be easily applied only on a series of VES soundings distributed on a given oriented profile.
   The superimposing of the results provided by applying the two mentioned approaches allows resistivity, thicknesses and structural model to be established along the studied profiles.

3. The third step is achieved by using the available geological information in order to finally establish a geological cross- section along the studied profiles.

Applicability of the described geoelectrical configurations is raised by the fact that they provide detailed tectonic information about shallow and deep pentration depths. The

advantages of such configurations are demonstrated through several field application examples presented with their analysis and interpretations. Therefore, the specific configuration with its particular shallow design is recommended to be applied for detecting and imaging faulted and fractured zones in Quaternary and Recent deposits and for exploration and mining geology, where shallow information depths are required.

## 3. Pichugin $ Habibulaev technique 1985

This technique is considered as the most sophisticated one for distinguishing tectonically fractured zones and oblique contacts between different rock types, and permits the determination of faults direction and dip amounts.

When an electrical current passes through a plane contact between two outcropping formations of different resistivities ρ1 and ρ2, (Fig.2) then electrical field boundary conditions at this contact, are characterized by the following:

- If the center of vertical electrical sounding is exactly located over a vertical contact between two formations of different resistivities ρ1, ρ2, and the configuration is perpendicular to this contact, then the resulting measured resistivity ρK is given by the following equation:

$$\rho K = (\rho 1 + \rho 2) / 2 \tag{3}$$

- and if the configuration is parallel to such a contact, then the resulting measured resistivity ρ'K is given by the following equation:

$$\rho' K = 2\, \rho 1\, \rho 2 / (\rho 1 + \rho 2) \tag{4}$$

In both cases, the resistivity does not depend on AB or MN lengths.

- If there are two vertical electrical soundings VES1 and VES2, performed on either side of a vertical contact, then all profiling curves for every given AB/2 will be intersected in one point located over this vertical contact. The data of vertical electrical soundings is therefore converted to be represented by the form of horizontal curves as multi-depths profiling curves for every given AB/2. The locations of vertical electrical soundings, realized on a given profile, are plotted on abscissa using a linear scale, while the corresponding apparent resistivities (ρK or ρ`K) for each given AB/2 are plotted on ordinate using a logarithmic scale. The intersection points of all horizontal curves termed as "Points of Non-Homogeneity", (PNH) and labeled by (+) symbol are plotted on a 2D (x, z) geological section. The depth z of each of them can be determined according to the following equation:

$$Z = [(AB / 2)_i + (AB / 2)_j] / 2 \tag{5}$$

Where $(AB / 2)_i$ and $(AB / 2)_j$ are the half separations between the electrodes A and B, for which two horizontal curves are intersected. The fractured zones are identified and determined by the presence of (PNH) on vertical pseudo vertical lines.

The geological interpretation of the PNH is based on the following assumptions:

- When the (PNH) are distributed according to the oblique lines located at shallow depths, they point to the presence of an inhomogeneous lithological contact;
- If they are arranged along oblique lines dipping down at an angle exceeding 30° in depth, they represent a tectonic fractured zone;
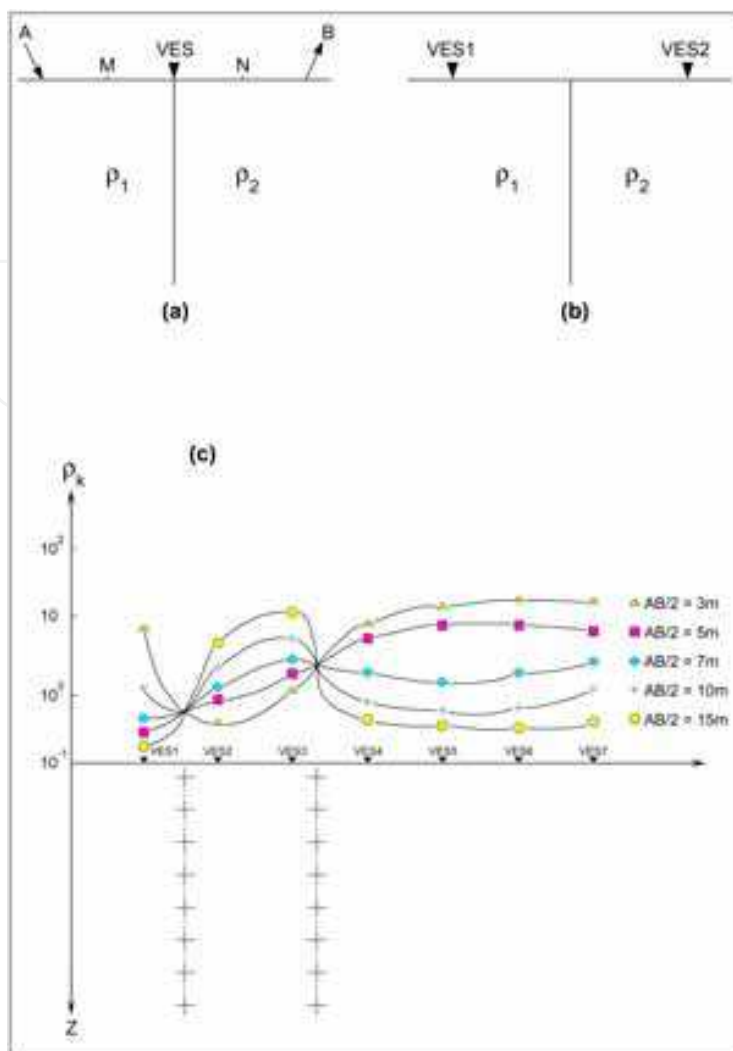
Fig. 2. The principle of Pichugin and habibuleav technique ( 1985).

- If they are randomly scattered near the surface, they indicate an homogeneous lithology;
- If they are arranged in a regular form, they reflect may be the presence of geological structures in the region of study (syncline, anticline, or simply horizontally layered strata).

More recently, Asfahani in the paper of Asfahani and Radwan (2007) enhanced the technique by taking into consideration the real topographic variations of the studied soundings (VES) distributed along a given profile, in order to accurately acquire reliable subsurface structures. This enhanced technique is widely used for identification of the subsurface tectonics as will be shown in the following five case problems presented in this chapter:

### 3.1 Characterizing the active tectonic of the Quaternary and Recent deposits in Al-Ghab depression region

Quaternary and Recent sediments represent indeed, a valuable record of the active tectonic events which have happened in the last 10.000 years. Being mainly composed of soft sediments covered usually by top soil, they are very susceptible to be weathered and eroded even in a short time, where their traces of surface expressions containing the records of the occurred tectonic deformation are partially or completely eradicated. Additional short term factors  that either damage, bury or wipe away the remaining rest of this natural record, are

represented by escalating diversified human activities, started from the dawn of civilization, ranging from land cultivation to giant dams construction.

The need to support the morphotectonic mapping of surface active tectonic features with subsurface data in order to acquire a reliable, intact, and well-preserved a 3-D image of Quaternary sediments deformation is one of the main challenge in active tectonic studies. The need to implement adequate methods able to provide a truthful insight in such sediments becomes more and more pressing.

Most of the geophysical methods used today in many applications have been invented and developed to meet the increasing demand of the society for new water, mineral and energy resources, which usually lie under considerable depth. Accordingly, geophysicists strive to devise much deeper-penetrating methods and contrive new data interpreting methods and models.

In active tectonic researches, the scope is reversed, since data on shallow depth subsurface structures are strongly needed to map and image the near surface fault trace with great accuracy.

Syria lies at the northern margin of the Arabian plate, and to the south of the East Anatolian Fault (EAF) that separates the Arabian plate from the Anatolian plate. The N-S trending Dead Sea Fault System (DSFS), which crosses through the western parts of Syria is a major sinistral transform plate boundary between the African (Levantine sub-plate) and the Arabian plates (Fig.3). It accommodates their differential movement, linking the Red Sea /
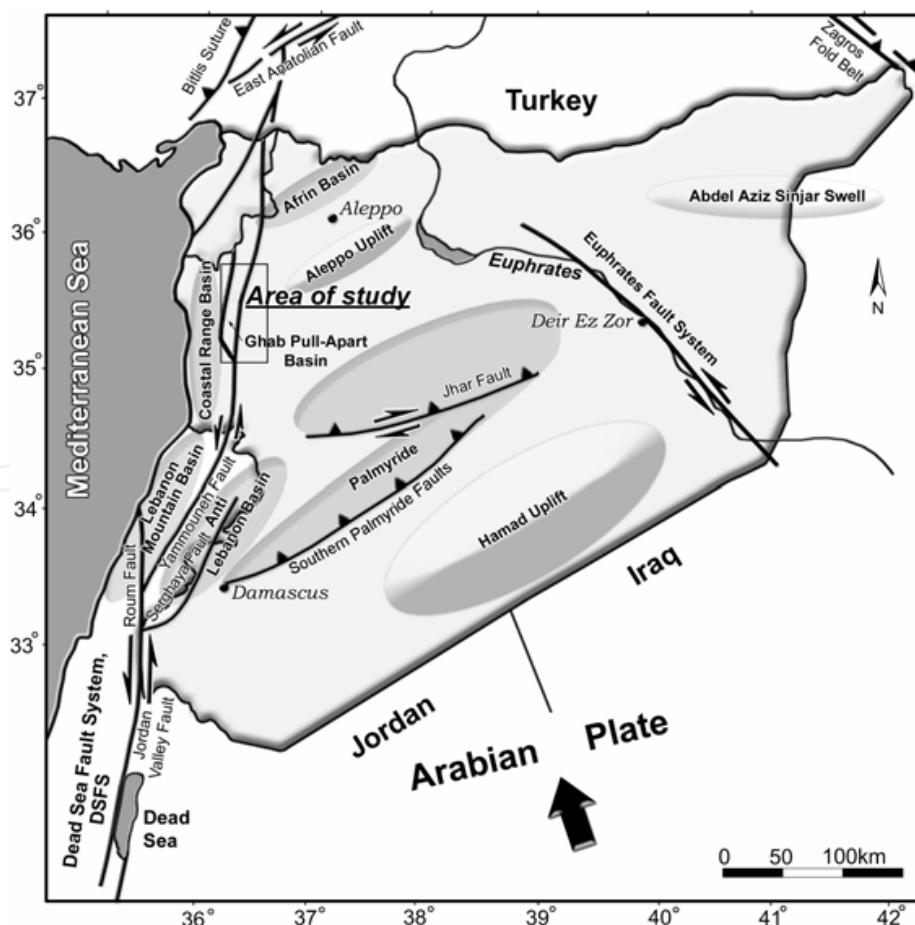


Fig. 3. The main tectonic features of Syria and the location of the study area.
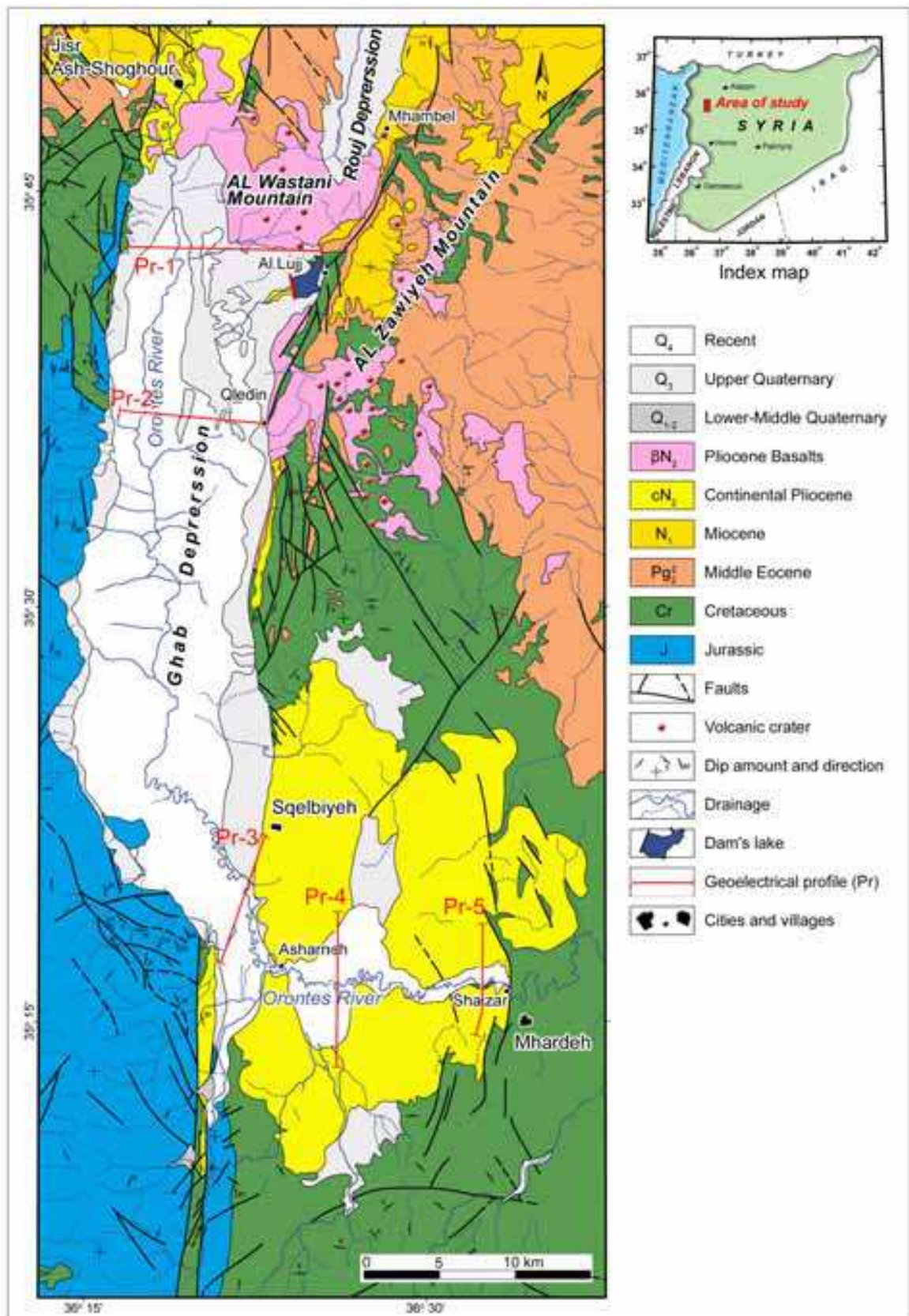
Fig. 4. Simplified geological map of the Al Ghab area, with the locations of the executed geoelectrical profiles.

Gulf of Aqaba seafloor spreading to Neo-Tethyan collision in Turkey, involving complex structural deformation controlled by the prevailing stress field along it.

Ghab rift valley is developed along the northern parts of the DSFS in Syria. Brew et al. (2001a, 2001b) consider this pull-apart basin as a deep structure opened in response to a left-step in the DSFS during Pliocene to Holocene. It is bounded from the north and northeast by the NNE elongated Al Rouj Valley and Al Wastani Mountain. It is separated from Al Zawiyeh Mountain to the east and from the Coastal Chain to the west by bounding linear faults and to the south by a NW normal fault, (Fig.4). The Ghab depression is filled by horizontal, 90-150 m thick Pliocene lacustrine sediments, covered by a thin sheet of Quaternary lacustrine sediments (Ponikarov 1966).

The Asharneh depression is of an elliptical shape, stretching in a meridian direction. It boards the Ghab depression from the East. The East of Asharneh depression is limited by a system of small echelon- like faults.

Pliocene continental deposits fill the tectonic basins of Ghab and Asharneh. It appears on the marginal edges of those tectonic depressions margin deposits in contact with the older rocks of different ages.

The Pliocene effusives composed of basalt and tuff cover have been developed in the northern part of the Ghab depression. The basalt cover is slightly inclined in southward direction, where it is buried under Upper Quaternary and Recent deposits.

Shallow and deep vertical electrical soundings (VES) have been applied in Al-Ghab depression region in order to characterize the Quaternary and Recent deposits.

More than 70 VES soundings distributed on five profiles are carried out, where the locations of those profiles are shown in Fig.4. The acquired VES data have been interpreted by the new proposed approach constructed by the three previously described steps. The second tectonic step which consists of finding the points of non homogeneity (PNH) is the most important in such a proposed approach, and allows the subsurface tectonic features along a given profile to be easily traced. This chapter shows just an example of the interpretation results obtained by applying the proposed interpretative approach on the shallow and deep Zaizon profile as follows:

### 3.2 Pr-1 shallow and deep  Zaizon profile

This profile of a length of 13 Km, was executed in E-w direction and has 13 VES data points. The interpretation of this profile by the new proposed interpretative protocol allows very detailed information to be obtained for the shallow depth not exceeding 50m as shown in Figure.5-a. In accordance with the available geological information and the multi-layer models obtained by the inversion, a geoelectrical cross section was established along this profile. The cross section revealed in general four to five layered subsurface mediums as follows:

- The first uppermost, geoelectrical layer is of a thicknesse varying between 0.3 and 1.8m, with an average thickness of 0.7m. It exhibits resistivity values ranging between 4.4 and 33 Ohm.m. It is composed of salty marshs and eolain sands.
- The Recent geoelectrical layer is relatively thin ( 0.8- 5.7m), and exhibits resistivity values ranging between 1.7 and 144 Ohm.m reflecting the effect of surface conditions and/ or the very lithological variations. It is composed of peat, clayey loams, sands, and pebbles.
- The Quaternary geoelectrical layer is relatively thin ( 15.5- 60m), and exhibits resistivity values ranging between 0.7 and 60 Ohm.m. It is composed of alluvium, proluvium, clay and lacustrine limestone.
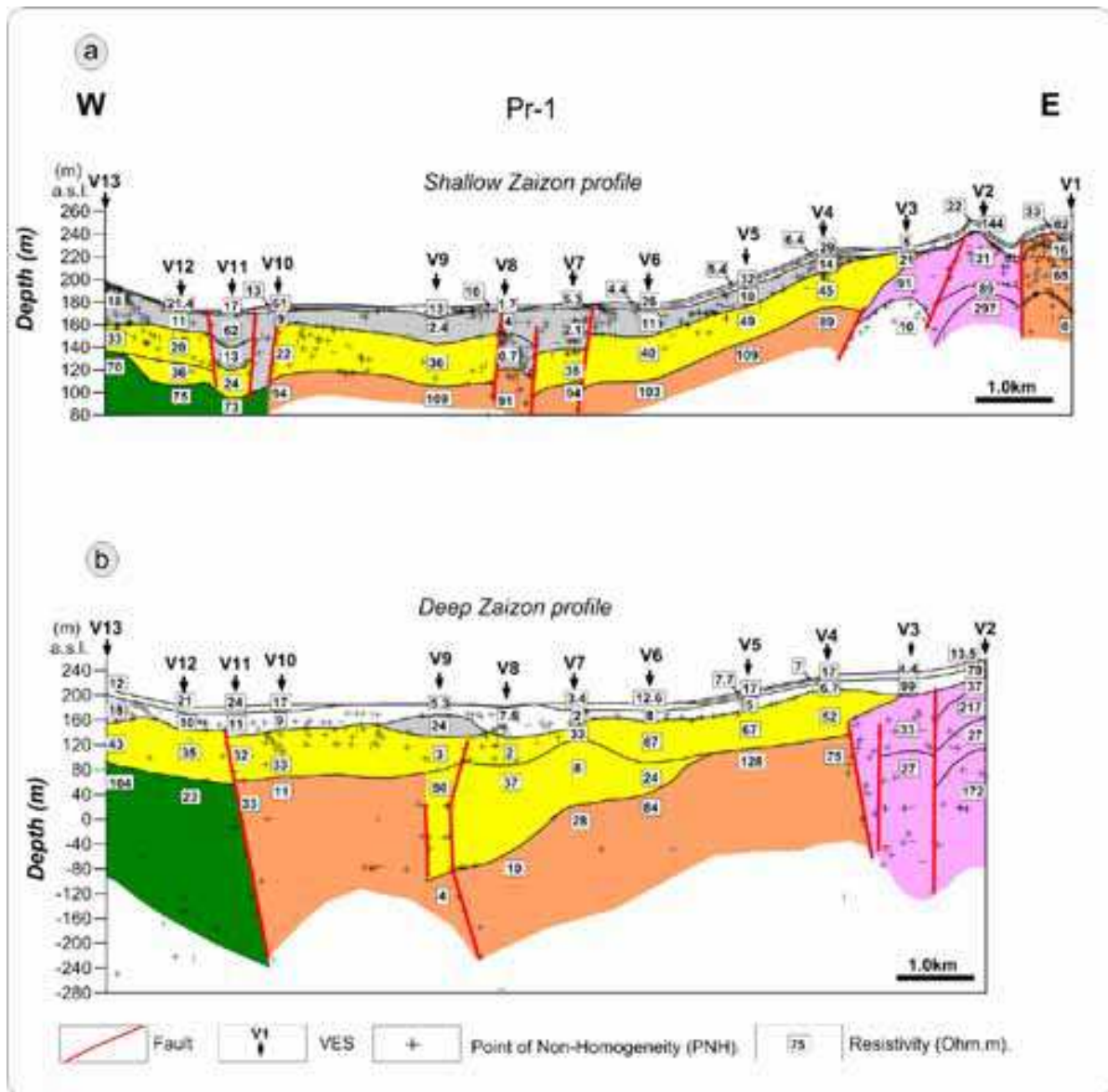
Fig. 5. Shallow and deep geoelectrical cross section on Pr-1 Zaizon profile.

The Neogene (Pliocene) geoelectrical layer is of a thicknesse varying between 2 and 31m with an average thicknesse of 24m. Its resistivity values are ranging between 21 and 49Ohm.m with an average of 35Ohm.m.

- The Neogene rocks are composed of lacustrine limestones, sandstones, coarse sands and conglomerates, and the effusive rocks which are composed of extinct volcanic vents filled with volcanic breccia and erosion product.
- The Paleogene geoelectrical layer is of a resistivity values ranging between 89 and 109Ohm.m with an average of 98Ohm.m. This Paleogene layer is shown between VES-4 and VES-10 (Fig.5). It is composed of clayey limestone, and organic limestone.
- The Cretaceous geoelectrical layer is of a resistivity values ranging between 70 and 75Ohm.m with an average of 73Ohm.m. This Cretaceous layer is shown only under the VES-11,12 and VES-13 (Fig.5). It is composed of blocks of limestone, dolomite, clay and flint.

The distribution of the PNH provides an idea about the subsurface structures and the sedimentological deposition along the studied profile. The boundary between the Quaternary and Paleogene geoelectrical layers is marked by the distribution of such points.

The positions of the faults along this profile have been well located. To the west of VES.2, one can easily notice the presence of a fault, which penetrates the Pliocene lava.

Three faults have been identified between VES6 and VES8, the first one nearest to VES7 cuts the Quaternary and Recent deposit cover. The second one located between VES7 and VES8 cuts only the Quaternary deposits. The third one beneath VES8 cuts the Quaternary and Recent deposits. The area between VES6 and VES8 could be considered as a faulted zone.

Another faulted zone composed of three faults is located between VES10 and VES12 and characterized by gradual decline, where a large thickness of Recent deposits have been accumulated as shown in Fig.5.

The interpretation of deep profile shown in Fig.5-b revealed the presence of the same detected layers described by the shallow array. The investigation depth obtained by applying the deep array is more than 250m, where a general description of the different geological layers is established, but there are no details about the Recent and Quaternary layers as obtained by the shallow array. The deep subsurface tectonic is also determined where the locations of the faults are also shown in Fig.5-b.

The fractured zones determined along shallow and deep profiles are in an acceptable concordance. However, some shallow faults are absent in the deep profile as shown under the deep VES7, where such faults only affect the shallow layers, or swallow up with each other along the deep profile as shown under the deep VES10 and VES11.

Similar results have been obtained while interpreting the other four shallow profiles (Qledin (Pr-2), Sqelbiyeh (Pr-3), Asharneh (Pr-4), and Shazar (Pr-5)), where the resistivities and thicknesses of the different geological formations have been well determined as shown in Table [1].

| Profile Name | Recent | | Qunternary | | Neogene | | Paleogene | | Cretaceous | |
|---|---|---|---|---|---|---|---|---|---|---|
| | AV Resis (Ohm.m) | AV Thickness (m) | AV Resis (Ohm.m) | AV Thickness (m) | AV Resis (Ohm.m) | AV Thickness (m) | AV Resis (Ohm.m) | AV Thickness (m) | AV Resis (Ohm.m) | AV Thickness (m) |
| Pr-1 | 44 | 1.6 | 12 | 29 | 35 | 24 | – | – | 73 | – |
| Pr-2 | 34 | 1.2 | 25 | 10 | 56 | 21 | 50 | – | 36 | – |
| Pr-3 | 25 | 6 | 20 | 17 | 27 | 31 | 53 | – | – | – |
| pr-4 | 40 | 3.5 | 18 | 27 | 21 | 16 | – | | – | – |
| Pr-5 | 22 | 2 | 34 | 9 | 32 | 20 | – | – | 190 | – |

Table 1. The geometric and resistivity characteristics of different geological ages along the five executed profiles.

### 3.3 Delineation of the impact of Ghab extensional tectonics on the Qastoon Dam in Northwestern of Syria

Zaizoon and Qastoon earth fill dams, distanced 5 km from each other at the northern parts of Ghab pull apart, were constructed during 1990-1996 and set in operation in 1996. Zaizoon dam collapsed in 2002, cosing 20 lives, flooding 5 villages and submerging 8,000 ha of fertile agricultural land.

The latent impact of the Ghab extensional basin tectonic setting, and associated deformations resulted by active tectonics on the Qastoon dam in northern Ghab in Syria

have been evaluated, (Asfahani *et al.*, 2010). This was achieved by applying an appropriate methodology essentially based on morphotectonic mapping and integrated geophysical surveys, consisting of electrical resistivity profiling, vertical electrical sounding and self-potential techniques. The integrated interpretation of the acquired morphotectonic and geophysical data allowed the detection of subsurface deformed structures, either underlying the Qastoon dam lake floor, or close to it. It is believed that these active structures were developed through the ongoing active tectonic processes occurring in the Northern Arabian plate. The tectonic survey proved that the N66.5°E striking Wadi Al Mashta fault, extending beneath the Qastoon dam lake floor, is one of the youngest active structures, and that the intersection of the fault with the Qastoon dam prism is a water-leaking point. Dam supporting measures, continuous monitoring and precautious disaster management are therefore recommended to be urgently adopted and practiced.

Asfahani in the paper of (Asfahani *et al.*, 2010) has applied the electrical resistivity profiling (ERP) to image faults and fractures for penetration depths ranging between 10 and 20 m,. The ERP was performed along two profiles at the Qastoon-Al Lujj site, the first one, labeled Pr-1, is 435 m long and oriented E21°S, the second one, labeled Pr-2, is 330 m long and E-W oriented (Figs. 6, 7a, and 7b). Traditional Schlumberger configuration with two fixed AB constant spacings of 30 and 60 m (Figs. 6, 7a, and 7b) was used for measuring the resistivity. A distance of 3 m between potential electrodes M and N is chosen. In fact, the choice of such current and potential spacings in this configuration has proven its efficacy in providing resistivity measurements from the required active tectonic depths. The computed geometric
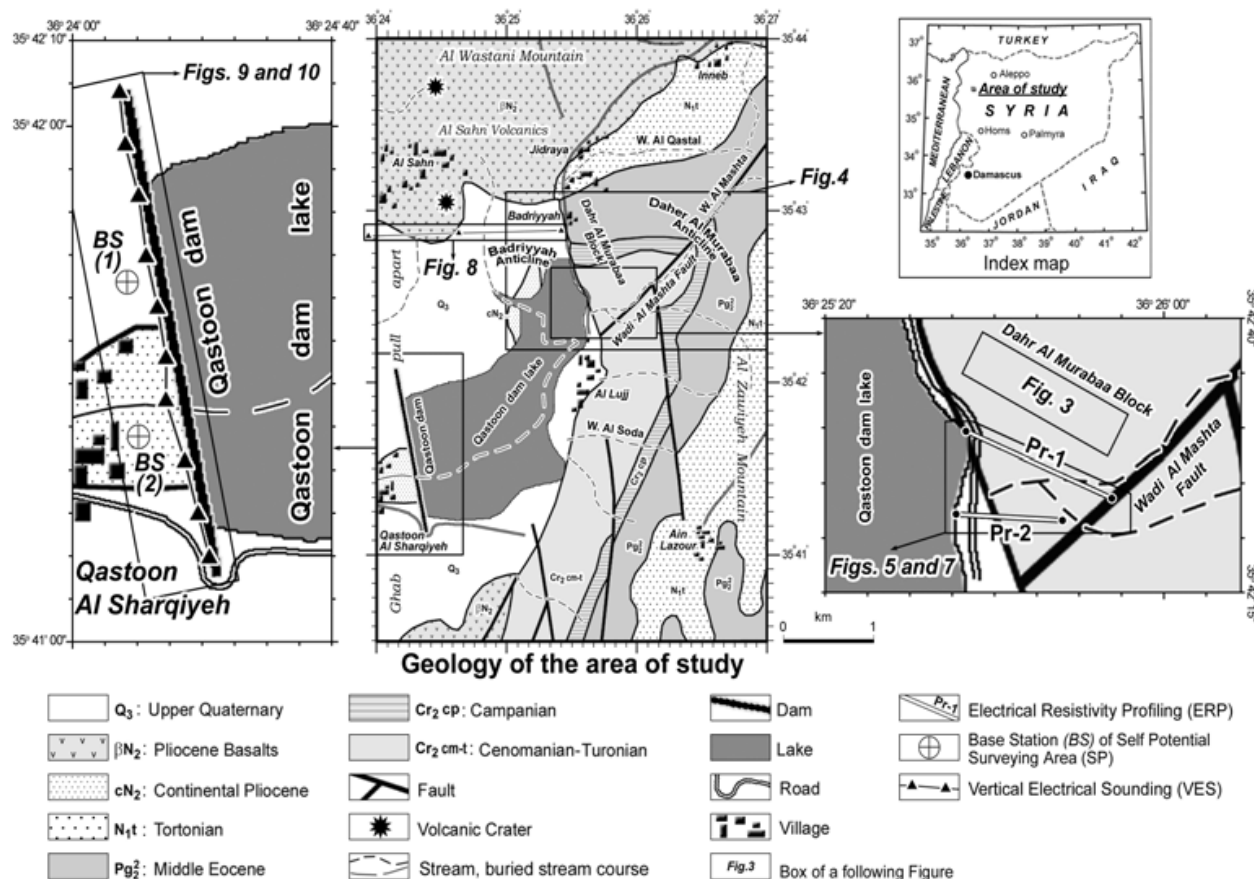


Fig. 6. Geology of the Al-Ghabe and location of Qastoon dam.
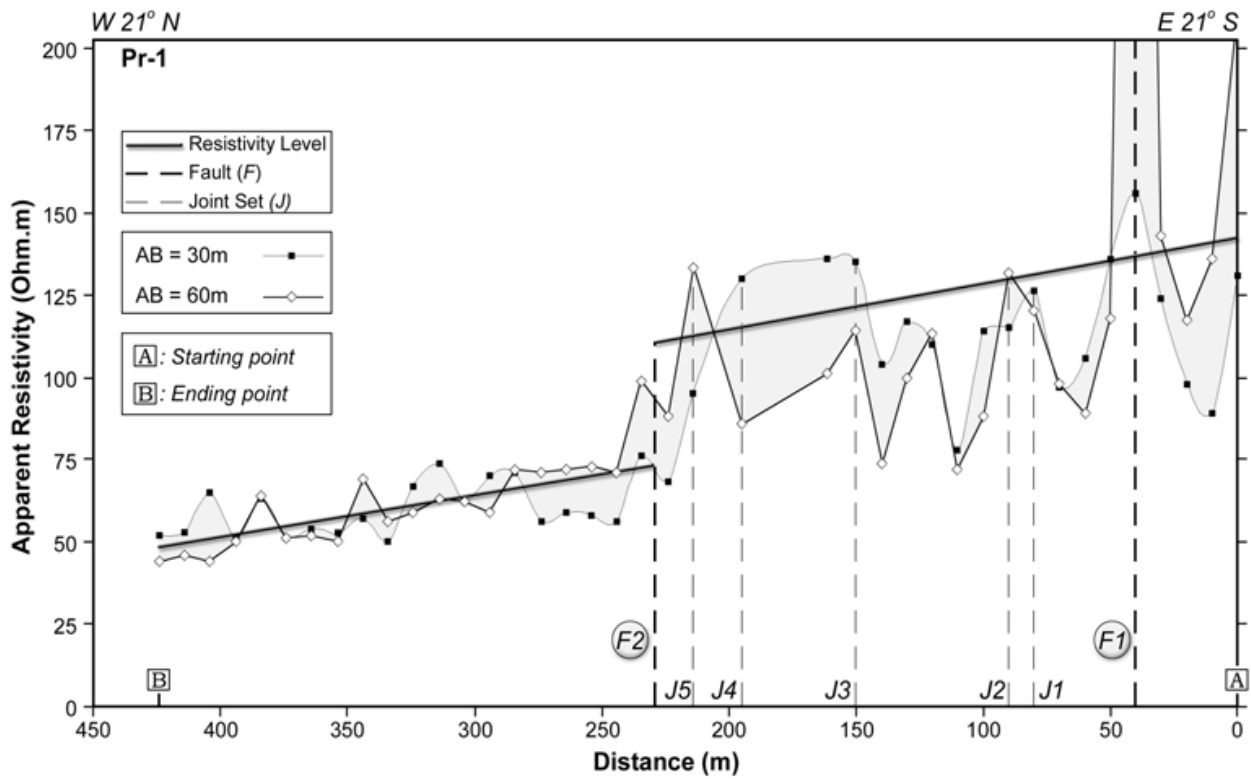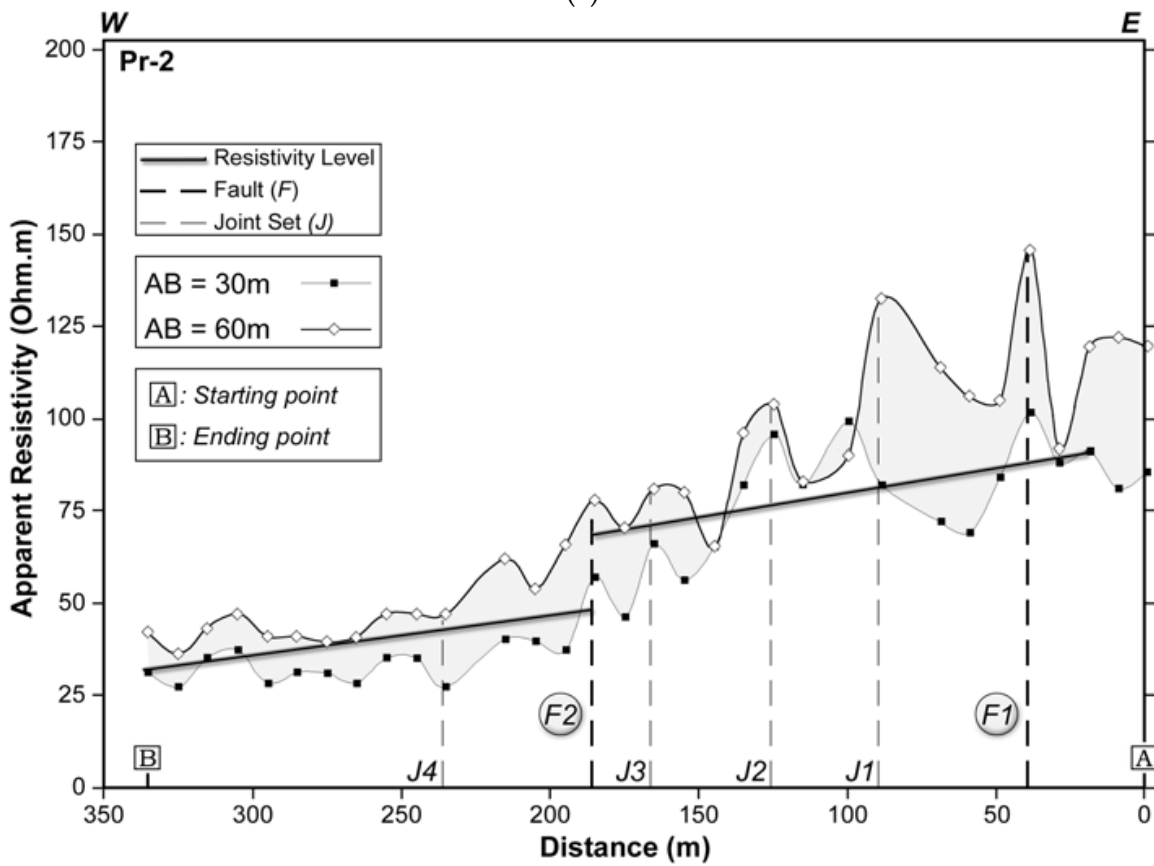
Fig. 7. (a) Apparent resistivity along Pr-1. (b) Apparent resistivity along Pr-2

The Role of Geoelectrical DC Methods in Determining the Subsurface Tectonics Features.
Case Studies from Syria

287

coefficients for AB of 30 m and 60 m are 233 m and 940 m respectively. Forty points along the Pr-1, and thirty two points along Pr-2, were measured with an interval of 10 m between every two successive measurements.

ERP was also carried out using Lee configuration to detect the locations of PNH which could be interpreted and attributed to the presence of faults and fractures. Lee configuration includes the use of five electrodes AMONB placed on a straight line on the ground (where OM=ON), as shown in Fig. 8.
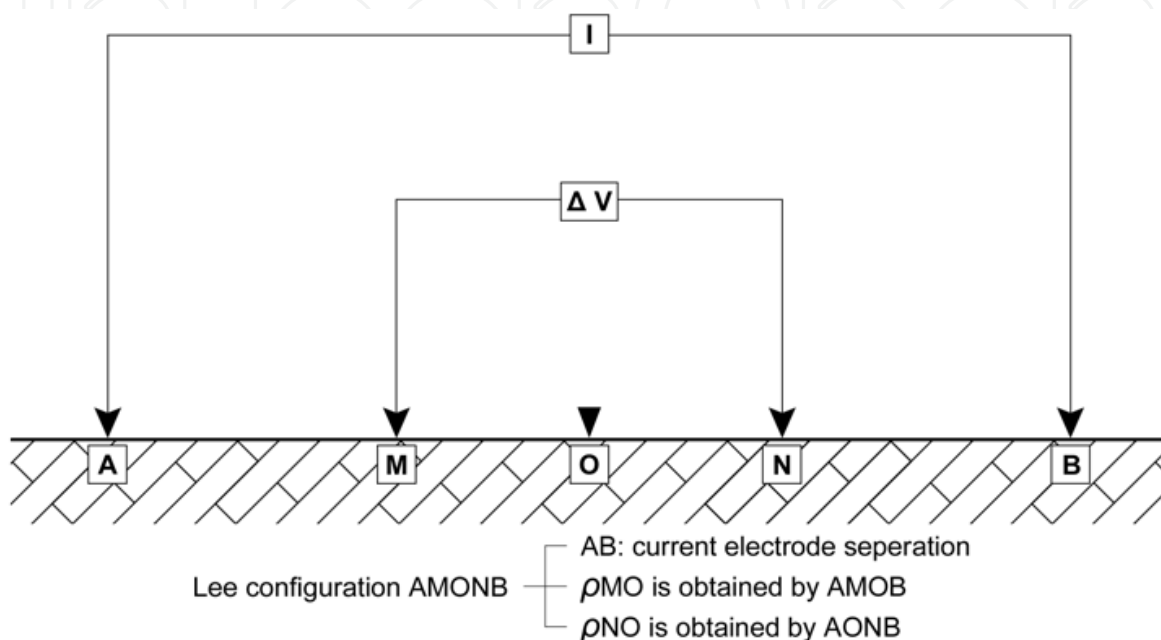


Fig. 8. Lee configuration in the field.

Three resistivities are measured by using such configuration as follows:

- Traditional $\rho a$ is results through A and B and measuring potential difference between M and N;
- $\rho_{OM}$ resistivity results through electrical current between A and B and measuring potential difference between M and O;
- $\rho_{ON}$ resistivity results through current between A and B and measuring potential difference between N and O.

The geometric coefficients of Lee configuration are computed for current electrode AB spacings of 30 and 60 m to be 466 m and 1880 m respectively, (the potential electrodes MN separation is constant and equals to 3m). The resistivity ratio variations $\rho_{OM}/\rho_{ON}$, for Pr-1 and Pr-2 profiles for both AB of 30 and 60 m, were followed, traced and interpreted (Figs. 9a, and 9b).

The tectonically-oriented interpretation of ERP (Pr-1) indicates the presence of two different apparent resistivity regions traceable at both 10 and 20 m penetrating depths for AB of 30 m and 60 m respectively (Fig. 7a).

- The first region extends 230 m westward from profile Pr-1, and is characterized by an average resistivity of ~130 Ohm.m. Within this region, a sharp resistivity peak (more than 200 Ohm.m). At 40 m from the profile starting point A, was interpreted as a sub-vertical fault (F1). Less pronounced resistivity peaks were interpreted as possible parallel joint sets (J).
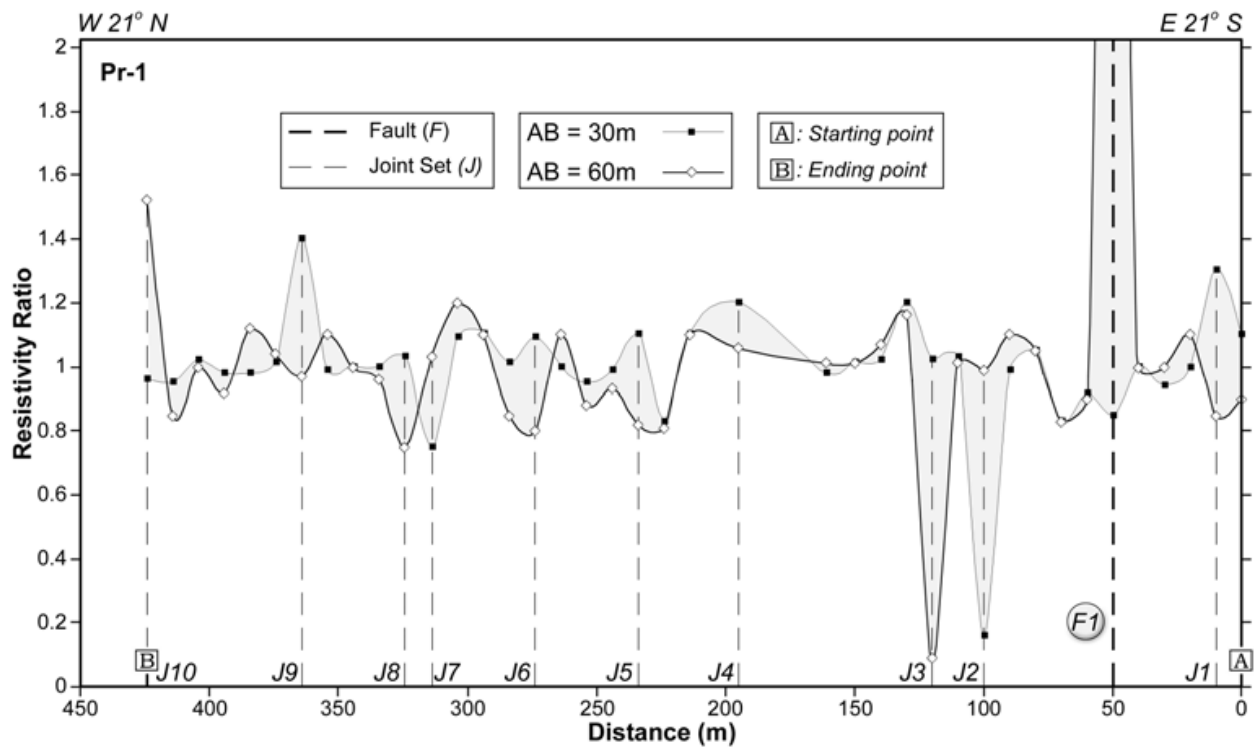
(a)
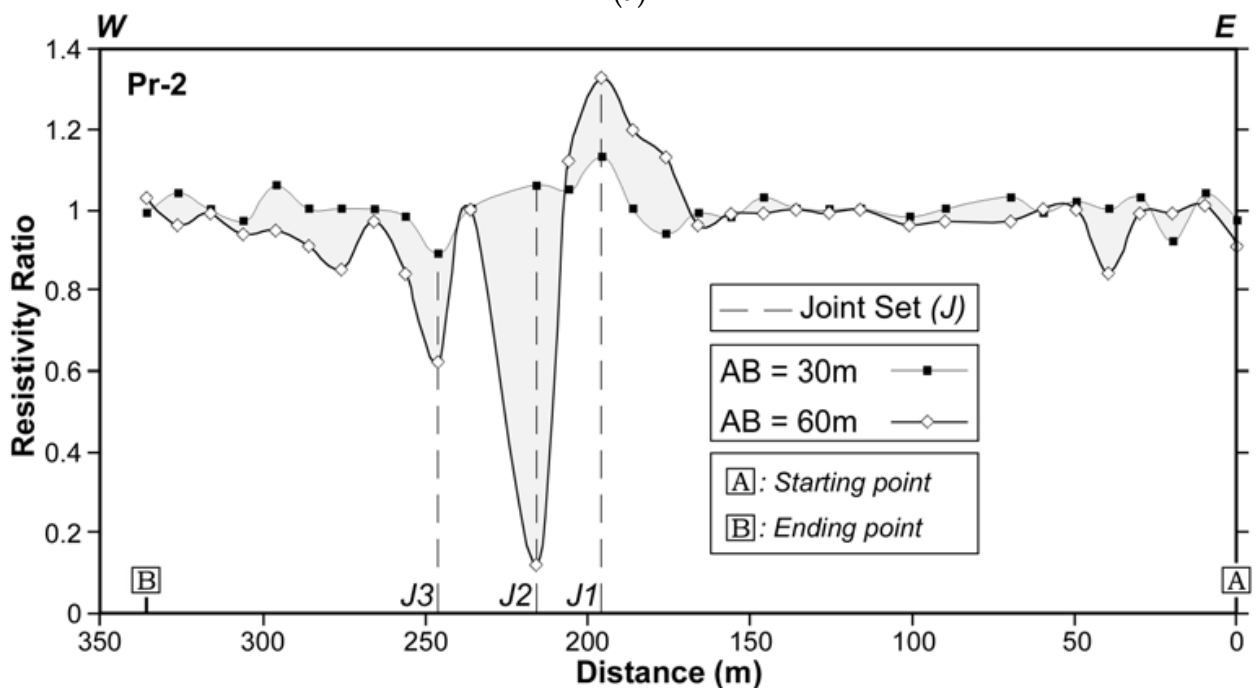


(b)

Fig. 9. (a) Apparent resistivity ratio along Pr-1. (b) Apparent resistivity ratio along Pr-2.

- The second resistivity region extends from the 230 m point on the profile to the profile endpoint B, with a 60 Ohm.m average resistivity. The deflection between these two resistivity levels was interpreted as another sub-vertical fault (F2). The weak resistivity peaks along this profile might be considered as minor deformational features.

Analysis of ERP (Pr-2) reveals a similar case, with two regions of average resistivities 75 and 40 Ohm.m values (Fig. 7b). The slope between them is traceable at both 10 and 20 m penetrating depths for AB of 30 m and 60 m respectively, marking a sub-vertical fault labeled (F2), distanced 185 m from the profile's starting point. A moderate peak is recognized in the 60 m-spaced AB, interpreted as (F1) fault distanced 40 m from Pr-2 profile starting point. Less pronounced peaks were interpreted as joint sets (J). F1 fault, traced on both profiles Pr-1 and Pr-2 was interpreted as the extension of the N66.5°E Wadi Al Mashta fault in depth, while F2 fault was interpreted as a parallel fault to F1.

*The interpretation of resistivity ratios profiles (Lee Configuration) is based on the studying of the* variations of the ratio $\rho_{OM}/\rho_{ON}$. As a rule, resistivity ratio value of $\rho_{OM}/\rho_{ON}$ = ~1, indicates an homogenous medium between M and N electrodes. Ratio values, deviating from 1, reflect a sharp geoelectrical contrast between adjacent media of different electrical characteristics, caused mainly by fractures and faults. Ratio variations and characteristics of Pr-1 and Pr-2 profiles were shown in Figures 9a, and 9b. The value that differs from 1 is interpreted accordingly as potential shallow active faults.

The interpretation of the *Badriyyah* VES profile by the inverse modeling revealed the presence of a lithological sequence that contains Middle Eocene chalky limestone and limestone, followed by Pliocene lacustrine marl and chalky limestone, caped by Pliocene basaltic flows and ending up by Quaternary alluvial sediments, (Fig.10). The interpretation of this VES profile by the Pichugin and Habibullaev method shows a clear deformation represented by faulting and folding of the previously mentioned sediments, where these results are in accordance with surface morphotectonic mapping. Integration of the results suggests the presence of a vertical, ~50 m deep normal fault, defining the western side of the 170 m wide Badriyyah graben. This finding is confirmed by the morphotectonic surface mapping of two normal faults striking N15°W and N15°E . Folding of the Eocene and Pliocene sediments, confined between the Badriyyah graben western fault and Al Sahn volcanics, have been observed through the interpretation of VES data. The interpretation findings were in concordance with surface morphotectonic field mapping that yields to detect the Badiryyah anticline (Fig. 10). The geoelectrical interpretation also detected faults that bound and penetrate Al Sahn basaltic volcanics, erupted high probably in Pliocene and post-Pliocene i.e. Quaternary, due to active tectonic processes.

The geoelectrical interpretation of Badriyyah VES profile confirms the presence of meaningful active tectonic deformation. The Badiryyah anticline and graben, folding and normal faulting of Pliocene sediments and normal faulting of Quaternary sediments those fill the aforesaid graben are evident examples of such deformation (Fig. 10). A southward draining paleo channel incising through them, and the presence of younger sediments burying this channel point to ongoing tectonics reflected by late steady subsidence of Badriyyah graben's central part, making it a potential water leakage site from Qastoon dam lake.

The interpretation of the N12°W shallow *Qastoon dam* VES profile of 1750 m long, measured parallel to the Qastoon dam, allowed the obtaining of a geoelectrical subsurface image beneath the dam prism (Fig. 11). It defined three pronounced spots with clear alignments of the Point of Non-Homogeneity (PNH) beneath V1, V5 and V8 soundings. The (PNH) alignment beneath V1 is relatively less significant since it lies beneath the dam northern end. The other two PNH alignments under V5 and V8 are alarming since they underlie the central part of Qastoon dam prism. They have been interpreted by considering the distribution of the measured resistivities values, as a SW extension of the NE striking Wadi
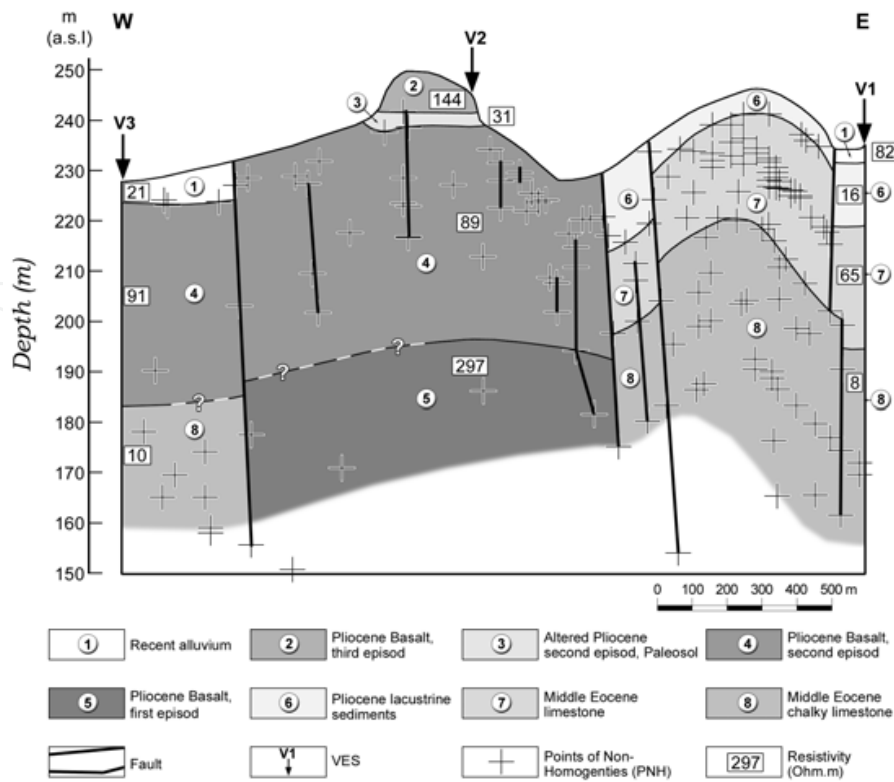
Fig. 10. Shallow subsurface geoelectrical cross section obtained along Badriyyah VES profile.
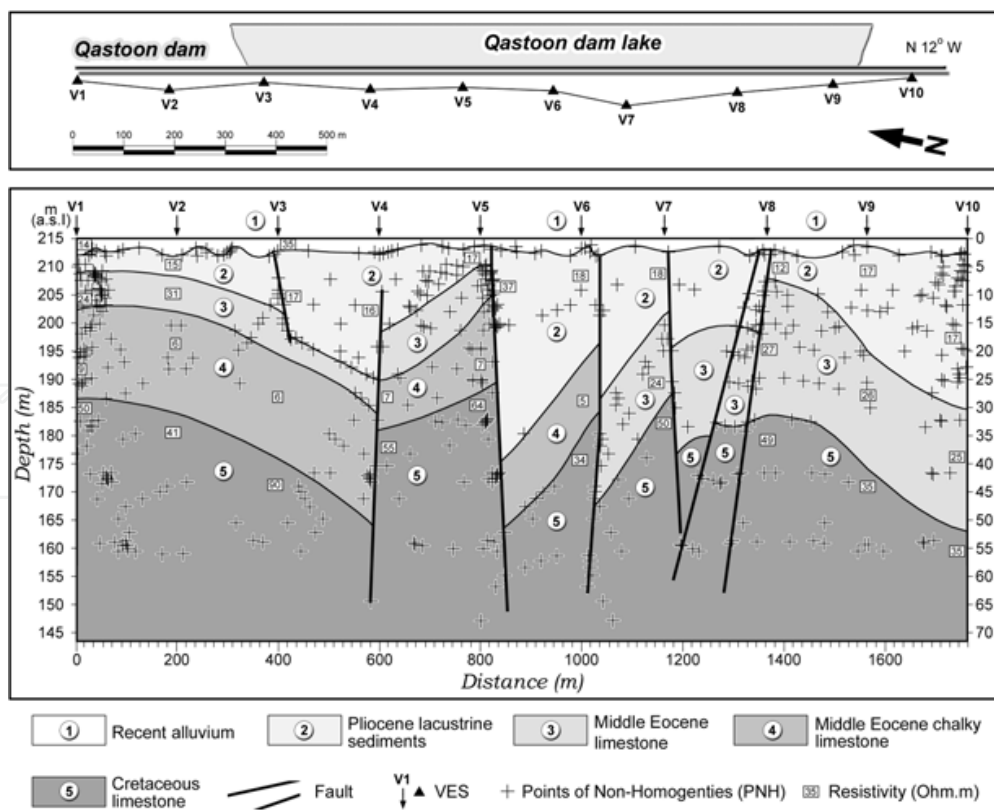


Fig. 11. Shallow subsurface geoelectrical cross section obtained along Qastoon Dam VES profile.

Al Mashta fault. Accordingly, V5 and V8 sites were selected to conduct Self potential (SP) measurements for detecting any possible water leakage at them from the dam lake. It is worth mentioning that after Zaizoon dam collapse, Qastoon Dam Monitoring Authority, installed 18 geodetic monitoring points on the dam prism and other 15 points at the dam's backside, to monitor land deformation in the area surrounding the dam. The authority conducts also continuous leveling using three-primary fixed benchmarks, seven secondary benchmarks and eight roving ones. Qastoon dam water controlling team, responsible for monitoring lake water level, spotted three water-leaking points. The first one is situated at the dam prism, the second one is located at the basaltic rocks that outcrop at the dam lake northern bank, while the third is located 200 m west of the dam. These observations are important, particularly the presence of the second leaking point, since it coincides with the N15°E striking normal fault, that defines the western border of the above mentioned Badriyyah graben. The first leaking point will be discussed while interpreting the SP data.
Two SP grids were established over area 1 and area 2, where the locations of V5 and V8 are respectively covered (Fig. 12). The map of SP for area 2 clearly reveals a distinguished N65°E SP elongated anomaly. The elongation axe is distanced 325 m from the southern end of the dam prism, and indicates a possible water leakage from Qastoon dam along it.
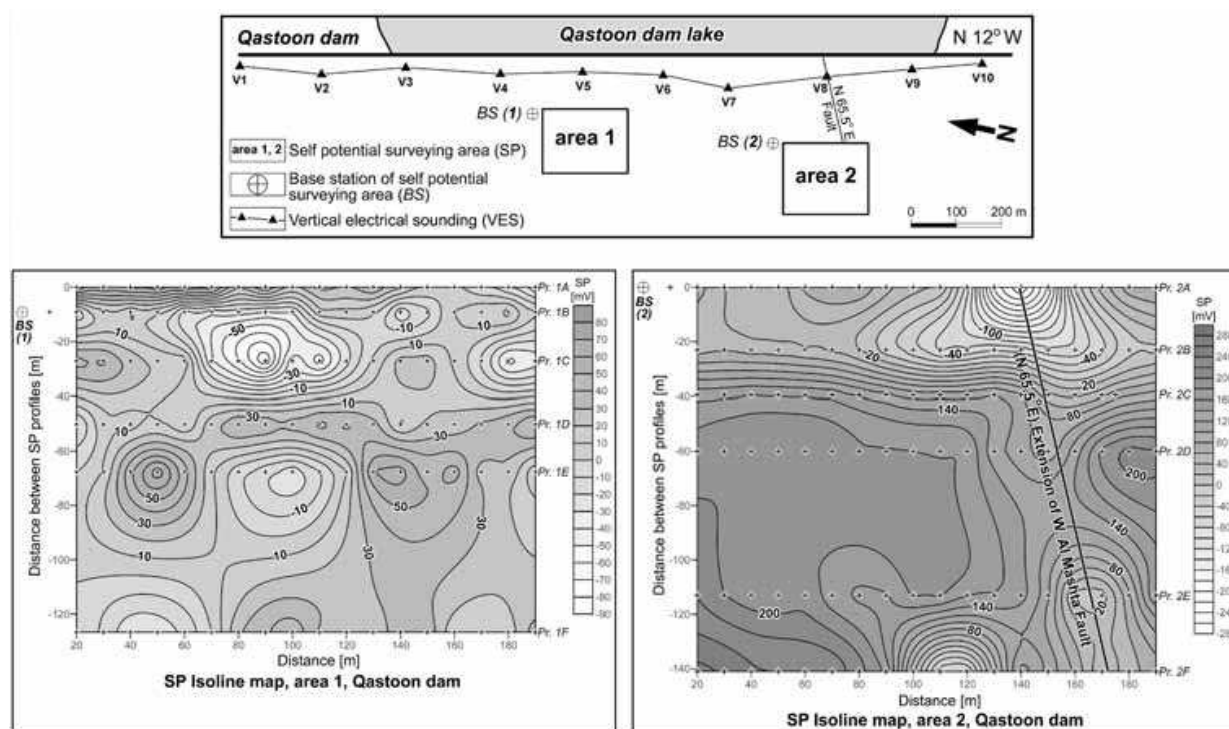


Fig. 12. SP maps in Areas 1 and 2 at the Qastoon Dam.

Remarkably, this elongation coincides with the direction of the NE striking Wadi Al Mashta fault. This strengthens the interpretation of a southwestern extension of Wadi Al Mashta fault beneath the dam lake's floor and the dam itself. Croot relationships, indicate that Wadi Al Mashta fault is either younger than the N15°W fault, which bounds the Badriyyah graben eastern end, or it is an older fault that than underwent a later reactivation. Accordingly, Wadi Al Mashta fault's formation and/or reactivation is indeed very recent, and its future reactivation is quite probable representing a real adjourned danger on Qastoon dam, ( Asfahani *et al.*, 2010).

The map of SP established in area 1 could be interpreted as shallow jointing set conjugate to Wadi Al Mashta fault (Fig. 12). The presence of 10° and 20° dipping Pliocene marly clay, clayey marl and clay horizons, forming the limbs of Badriyyah anticline, are hazardously lubricant horizons able to trigger slumping within Qastoon dam lake in response to a probable future earthquake. This bears an additional latent danger pending on Qastoon dam itself and on the surrounding villages.

### 3.4 Delineation of the tectonic of the Khanasser Valley in Northwestern of Syria

In Khanasser valley, considered as a semi arid region in Syria, the shallow groundwater presents electrical conductivities ranging from 0.1 to 20 mS/cm. In order to study the hydro geological conditions of such region, a good knowledge is required of the geometry of the aquifer at depth.

Khanaser Valley was therefore geoelectrically thoroughly surveyed through a grid consisted of twelve VES profiles as shown in Figs, 13, and 14). The tectonically-oriented Pichugin & Habibullaev method was enhanced to be applicable in areas of rugged relief and topography. The enhanced profiles were tectonically interpreted and subsurface structures within Khanaser Valley were delineated. Accordingly, a tectonic evolutional scenario of the valley was established and its hydrogeological characteristics were derived.

The established iso-apparent resistivity maps for different AB/2 depth penetrations indicate the presence of two different geological structures; characterized by very conductive zones of a resistivity less than 4 Ohm.m related to the intrusion of salt water in Quaternary and
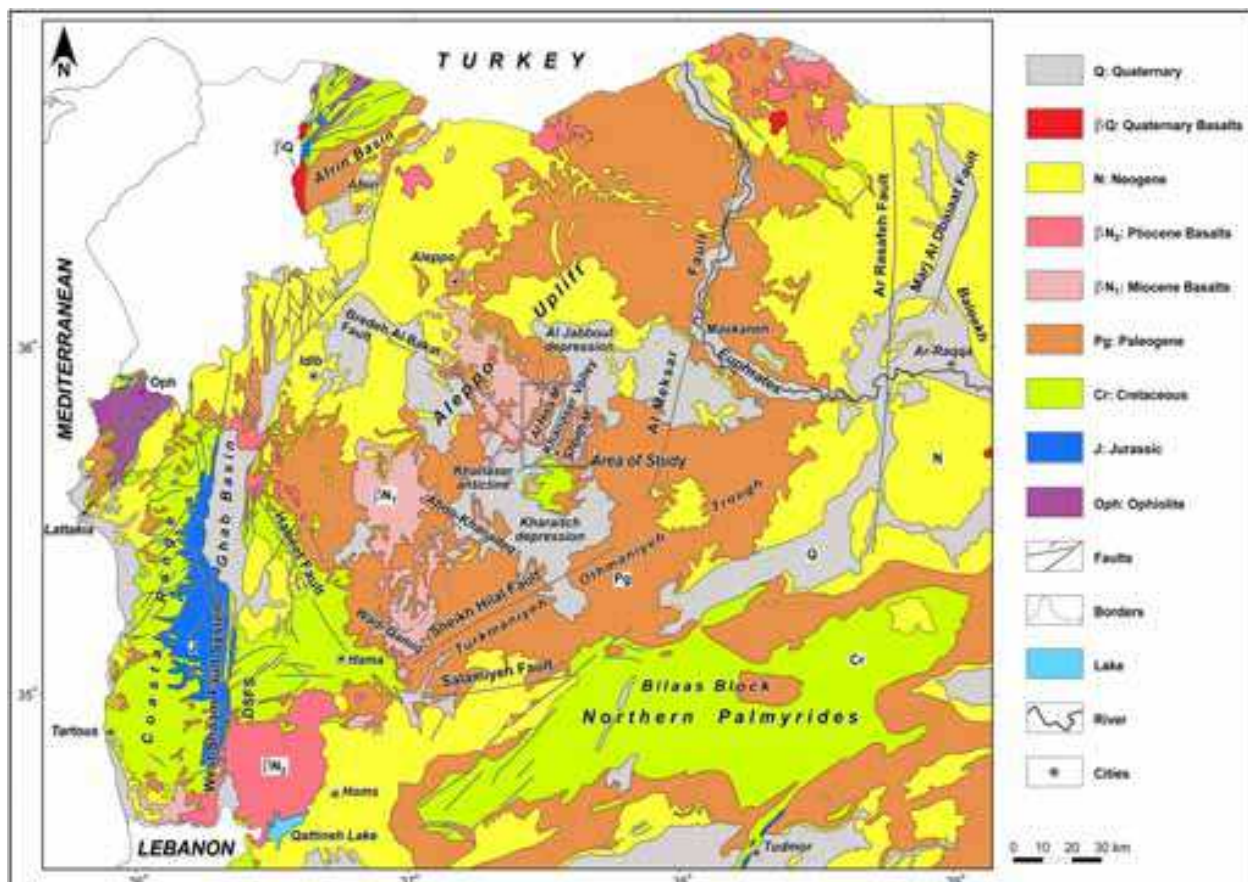


Fig. 13. Location of the Khanasser Valley.

The Role of Geoelectrical DC Methods in Determining the Subsurface Tectonics Features.
Case Studies from Syria

293
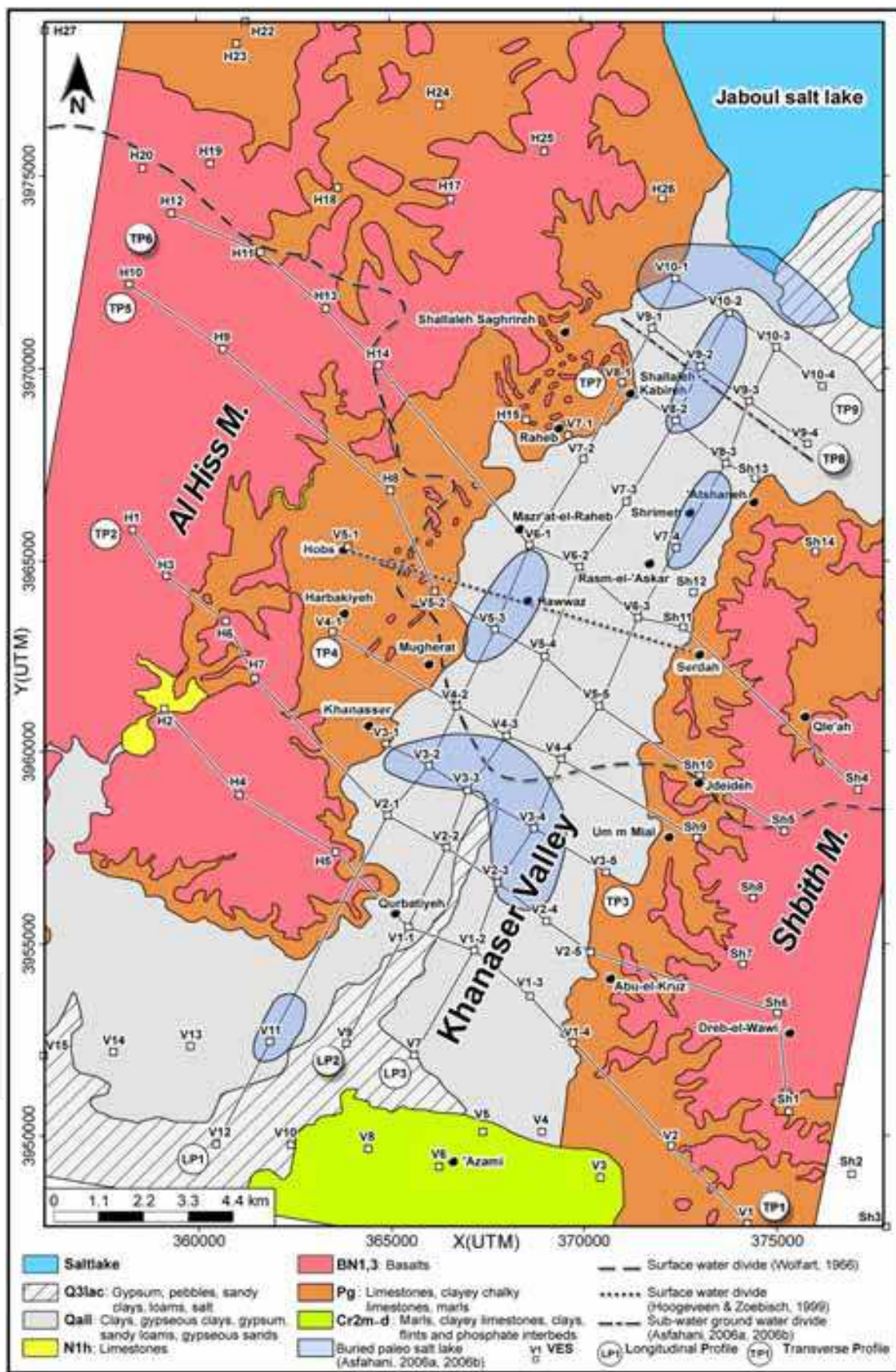


Fig. 14. Geology of the Khanasser Valley with the location of measured VES profiles.

Paleogene deposits. Resistive zones have been signaled in Jebel Al Hass in the west and Jebel Shbith in the east, characterized by a resistivity exceeding 300 Ohm.m, due to the presence of basalt formation of "BN1" age. The thickness of Quaternary, Paleogene and their electrical characteristics have been precisely determined. The top of Maistrechtian and its electrical characteristics have been also well established, Asfahani, 2007-a. Quaternary paleosabkhas were delineated through the studying of three longitudinal profiles a long the valley itself (LP1, LP2, and LP3), Asfahani, 2007-a.

Figures.15 and 16 show just two examples of the results interpretation of the transverse cross-section TP1 and TP6 by the application of both traditional and enhanced Pichugin $ Habibulaev method. The results of this interpretative method are presented by the PNH (+), which mainly show the locations of fractured zones. A clear concaved shape of the (+) with a width of 7Km was observed along the profile TP1 west of the Qurbatiyeh village. Clear normal faults, underlying the concaved shape bound sharply the Khanasser valley, and the field check confirms the presence of a volcanic crater to the northwest of Qurbatiyeh village, (Asfahani and Radwan, 2007).



Cultivated maar sediments of the Qurbatiyeh volcanic crater.

Inclined layered basalt at the rims of the Qurbatiyeh volcanic crater.
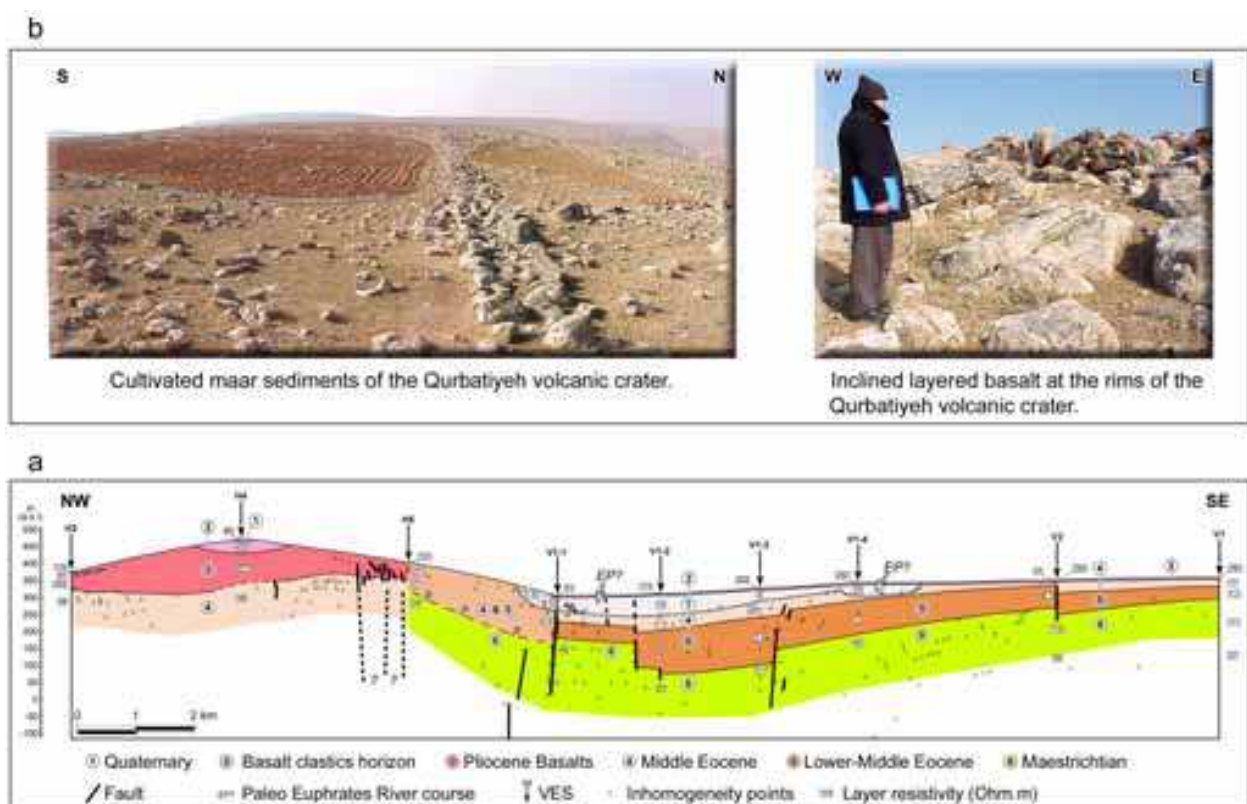
Fig. 15. Interpretation of transverse TP1 profile in the Khanasser Valley.
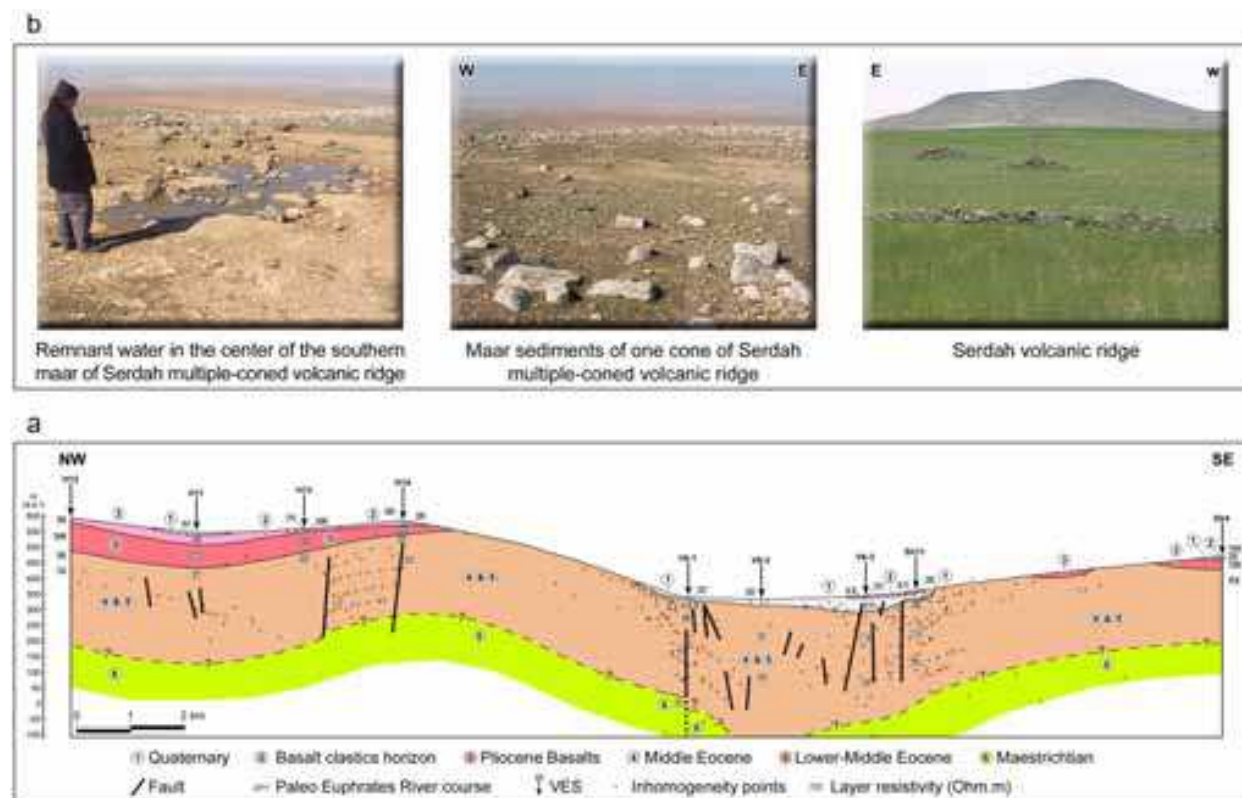
Fig. 16. Interpretation of transverse TP6 profile in the Khanasser Valley.

## 3.5 Application of the adapted shallow geoelectrical configuration in exploration and mining geology of phosphate deposits

The phosphatic deposits in Syria are actually mined in two main locations, Khneiffis and Al-Sharquieh phosphate mines as shown in Fig.17-a.

The Al-Sharquieh mine develops gradually to the south and southwest, where the phosphatic layers are approximately deposited in a horizontal position.

The geoelectrical and radioactive signatures of phosphate deposits in Al-Sharquieh mine in Syria have been identified through an extensive research work already published, (Asfahani and Mohamad, 2000). During this work, different geoelectrical methods have been successfully introduced and advised to be applicable while prospecting for phosphate resources.

The lithological and radioactive data of more than 40 drilled pits are used together in order to support the results obtained by the application of geoelectrical methods, where the location of those pits is shown in Fig.17-b.

On each of the drilled pits, a shallow vertical electrical sounding has been already carried out, where a total of 45 VES distributed on a regular grid was interpreted. The same VES measurements have been recently reinterpreted in order to clarify the subsurface tectonics, where seven field examples have been herewith presented with their interpretation, (Figs. 18, and 19), Asfahani, 2010-b. The structural picture of the study region has been well established, where a geoelectrical properties difference between Northern west and Southern east directions has been noticed. The Northernwest direction is characterized by uplifting structure where phosphatic beds are exposed at or near the surface. Profile-4 obviously shows this uplifting structure which is well indicated by the PNH distribution.
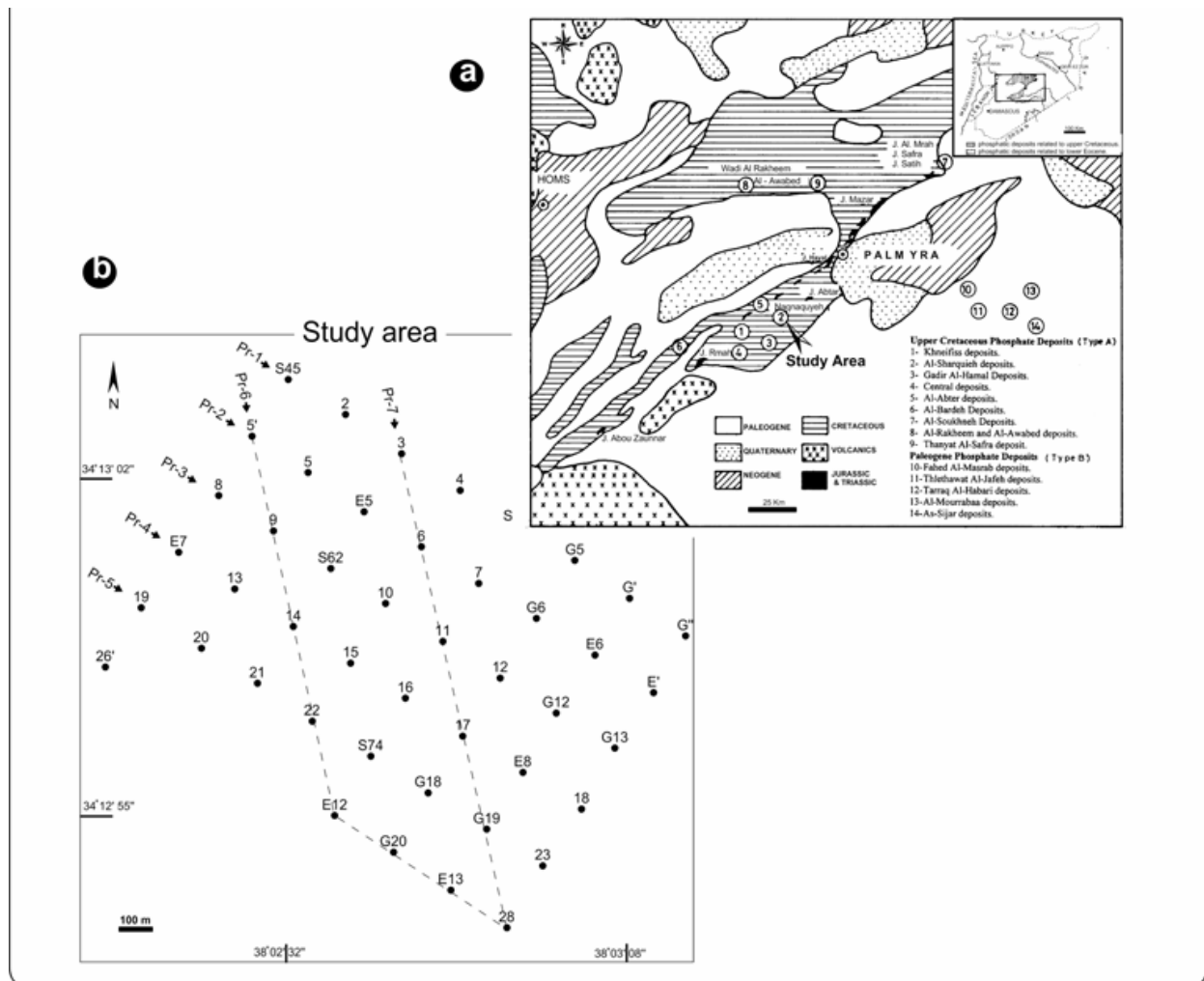
Fig. 17. a: Geology of the phosphate mines in Syria. b: Location of VES profiles in Al-Sharquieh mine.

The Southern east direction is characterized by low resistivity values and deepening of the phosphatic layers which deposited in a negative topographic structure such as subsiding sedimentary basin. This basined structure is beautifully indicated by the non homogeneity points distribution while applying the technique of Pichugin$Habibulaev (1985). The very condense clustering of non homogeneity points observed in many locations along the most of the studied profiles at depths ranging between 5 and 15 m are due to rapid lateral lithological variations normally observed in such sedimentological environments. The distribution of non homogeneity points largely contributes in delineating the positions of the faults in both Northwest and Southeast directions. The locations of the identified faults are characterized by high radioactivity due to the uranium concentrations in the phosphatic rocks. It appears quite clear that the maximum uranium concentration is confined to zones of tectonic weakening and to zone of fracturing.
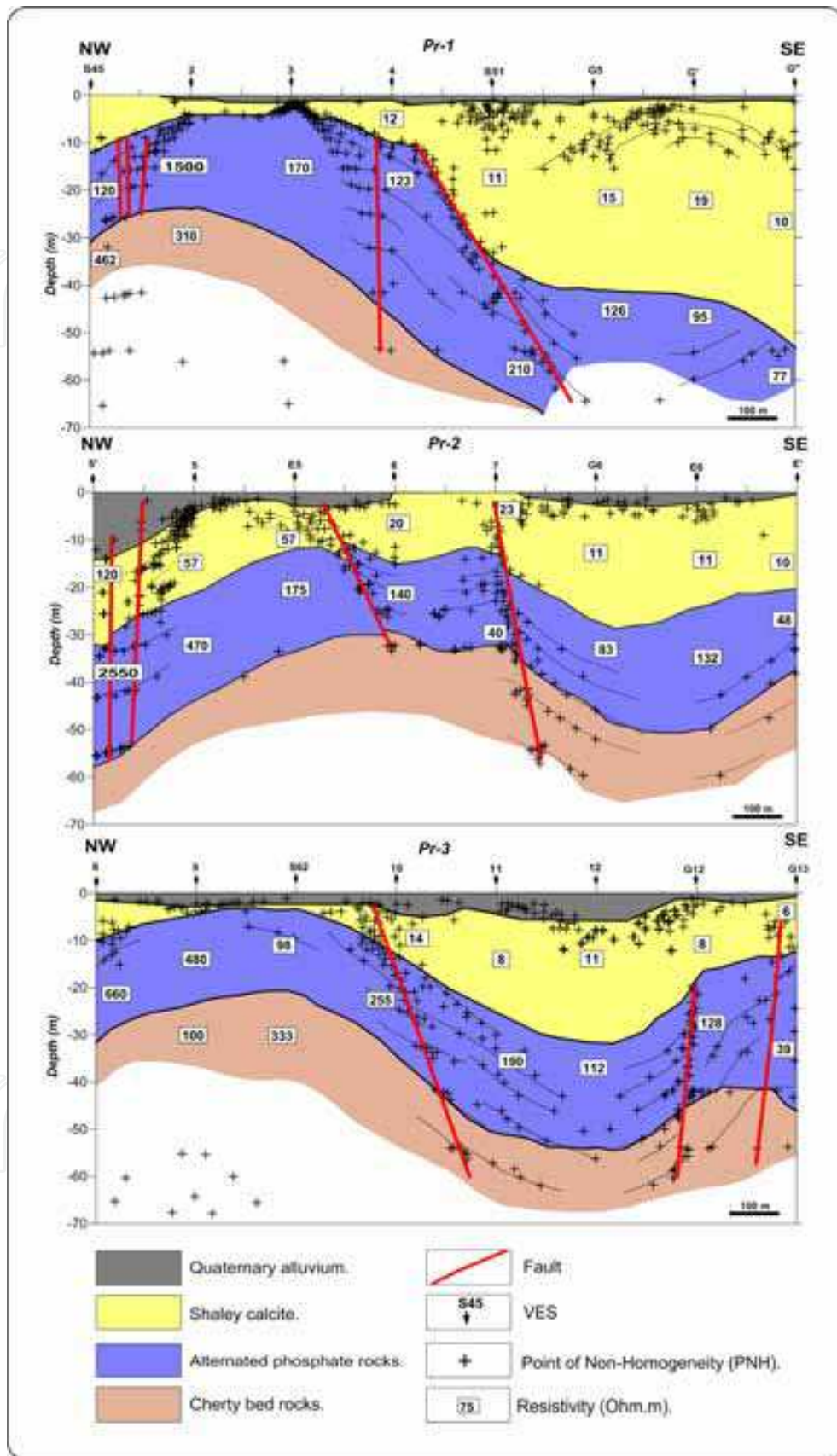
Fig. 18. Interpreted geological cross-sections of Pr-1, Pr-2,Pr-3 and Pr-4.
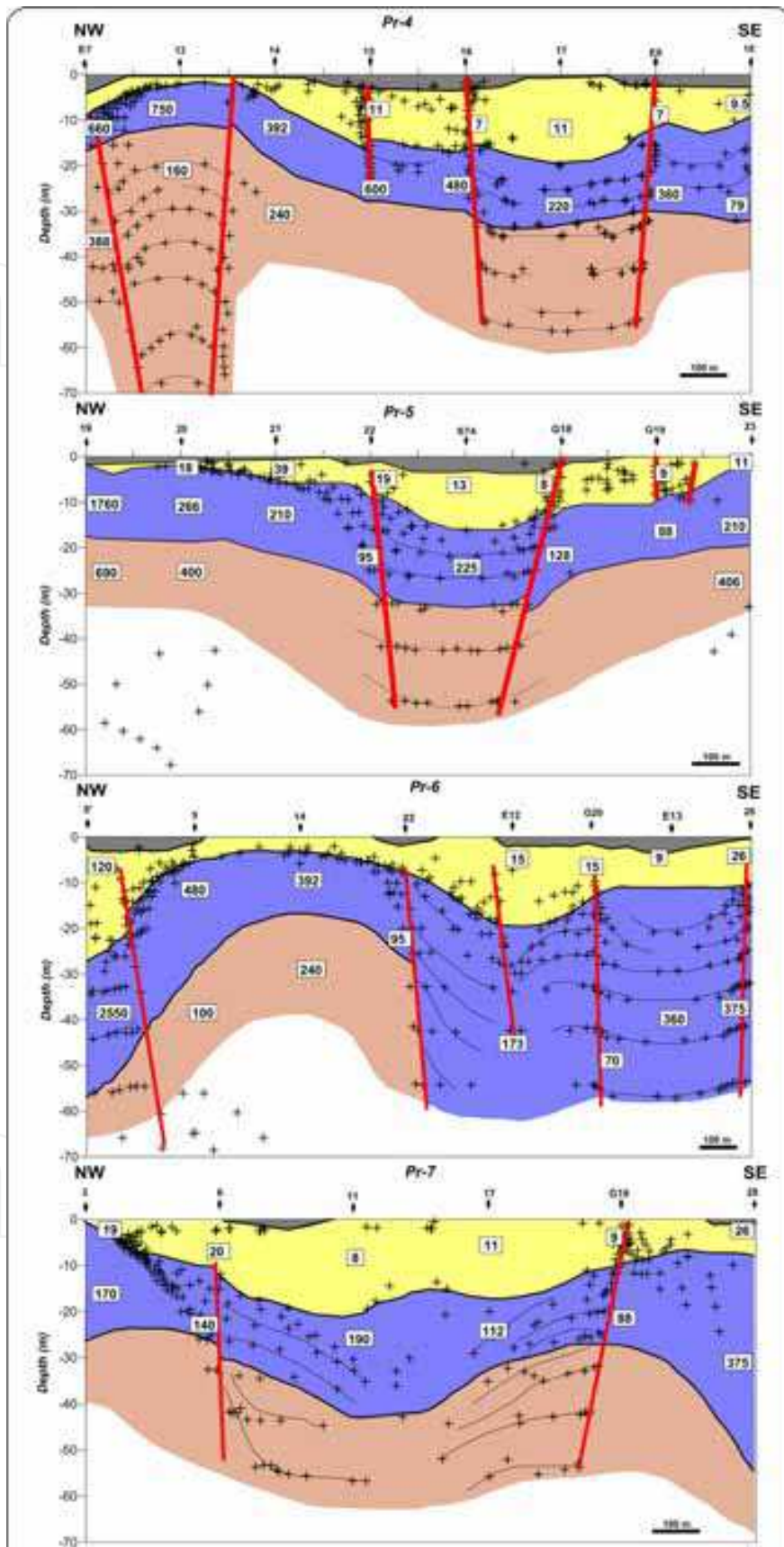
Fig. 19. Interpreted geological cross-sections of Pr-5, Pr-6, and Pr-7.

The Role of Geoelectrical DC Methods in Determining the Subsurface Tectonics Features.
Case Studies from Syria

299

## 4. Application of deep Schlumberger configuration in Northeastern of Syria for the *determination of the favorable structures for sulpher prospecting*

Electrical and structural characterstics of formations favorable for sulpher occurrence in northeast of Syria are described using geoelectrical prospecting methods. Simple (VES) and combined (CVES) Schlumberger vertical electrical soundings and geoelectrical profiling using Wenner configuration were applied to Techreen structure, Asfahani and Mohamad, 2002. The geoelectrical research has been concentrated on the studying of six profiles (A,B,C,D,E, and F) shown in Fig.20 and located at the borders of anticlines, where positive and negative structures are joined and salt formations have a tendency to disappear. Secondary structures characterized by high apparent resistivity exceeding 3000Ohm.m were located at each of the studied profil using Wenner profiling configuration. These secondary structures are demonstrated to be favorable for sulpher prospecting by both drilled wells and vertical electrical soundings. More than 84 VES measurements were carried out in the study area, where thicknesses and resistivities of the Lower Al-Fares, Al-Garibeh and Al-Dibbaneh formations were determined. The interpretation of those VES distributed along the studied profiles by the Pichugin $ Habibulaev technique allows the subsurface tectonic to be precisely determined for a depth penetration corresponding to AB/2 of 1000m. Figure.21 shows a beautiful example of such results interpretation carried out along the profile A. It was found that sulfur occurrences in the research area are controlled by tectonic paths that are well defined by geoelectrical methods.
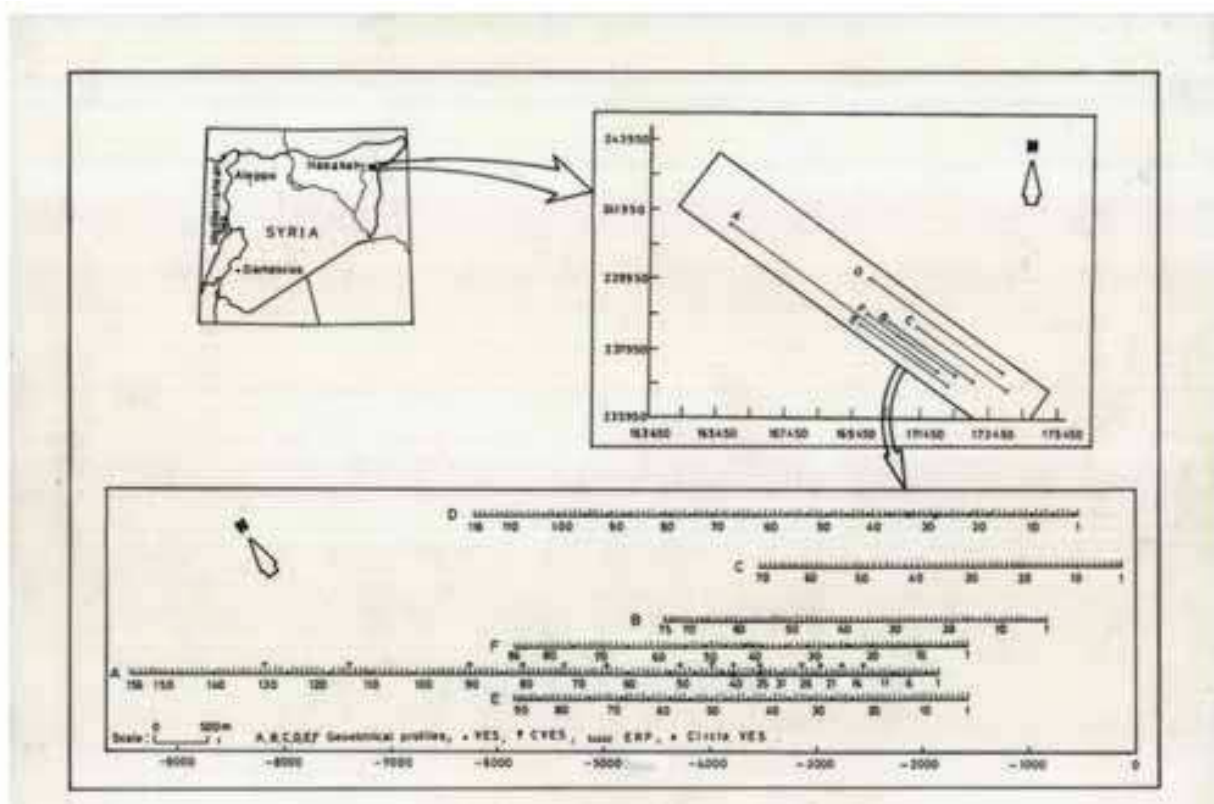


Fig. 20. Location of Techreen structure for sulpher prospecting.
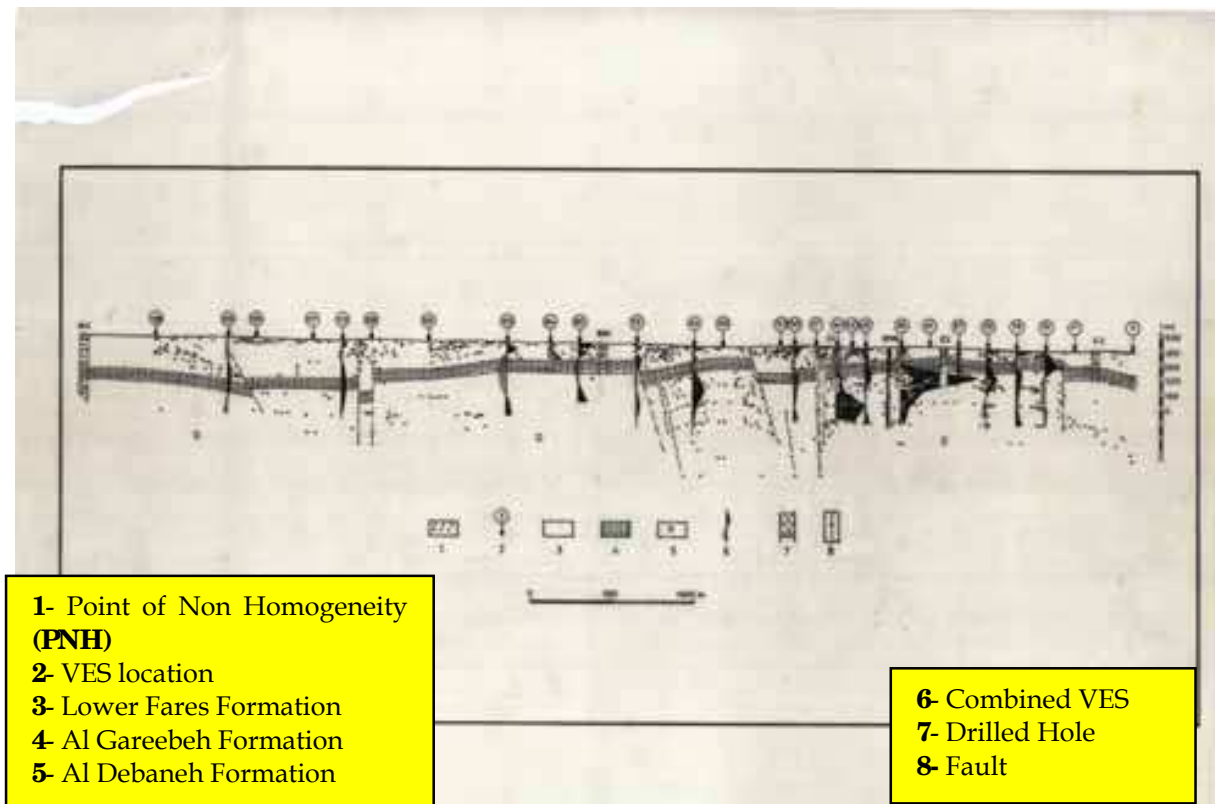
Fig. 21. Interpretation of VES distribution along profile-A.

## 5. Conclusion

Useful and important applications of the geoelectrical methods in delineating the subsurface tectonics features for solving different geological problems from Syria have been presented. The DC geoelectrical resistivity Schlumberger configuration is mainly developed and modified in order to simultaneously obtain reliable data for the shallow and deep penetration depths. The interpretation of the VES data by the enhanced Pichugin $ Habibulaev technique allows an integrated subsurface tectonic to be established along the studied VES profile, where typical selected examples have demonstrated the efficiency of such an interpretative technique and the role of DC geoelectrical methods in determining the subsurface tectonic features. This integrated interpretative technique with the application of modified Schlumberger configuration is therefore strongly recommended when tectonic subsurface information is required.

## 6. Acknowledgment

## 7. References

Asfahani, J. (2007-a), Geoelectrical Investigation for Characterizing the Hydrogeological Conditions in Semi Arid Region in Khanasser Valley, Syria. Journal of Arid Environnments 68, PP 31-52.

The Role of Geoelectrical DC Methods in Determining the Subsurface Tectonics Features.
Case Studies from Syria

301

Asfahani, J. (2007-b), Electrical Earth Resistivity surveying for delineating the characteristics of ground water in semiarid region in Khanaser Valley, Northern Syria, Hydrological Processes 21, 1085-1097.

Asfahani, J. (2010-a), *Electrical Resistivity Investigations for Guiding and Controlling Fresh Water Wells Drilling in Semi Arid Region in Khanasser Valley, Northern Syria, Accepte for publication in Acta Geophysica.*

Asfahani, J. (2010-b), A New interpretation approach of shallow and deep geoelectrical configuration for application in tectonic and exploration mining geology, Submitted for publication in Exploration and Mining Geology.

Asfahani, J., and Radwan, Y. (2007), Tectonic Evolution and Hydrogeological Characteristics of Khanaser Valley, Northern Syria, Derived from the Interpretation of Vertical Electrical Soundings, Pure Appl. Geophys. *164*, 2291-2311.

Asfahani, J., Radwan, Y., and Layyous, I., (2010), Integrated Geophysical and Morphotectonic Survey of Impact of Ghab Extensional Tectonics on the Qastoon Dam, Northwestern Syria, Pure Appl. Geophys. *167*, 323-338.

Asfahani, J., Mohamad, R. (2000), Investigation of electrical properties of radioactive phosphatic layers in Al-Sharquieh mine, Syria, Exploration and Mining Geology., Vol.9, 141-148.

Asfahani, J., Mohamad, R. (2002), Geoelectrical Investigation for sulfur prospecting in Techreen structure in northern Syria, Exploration and Mining Geology., Vo.11, 49-59.

Brew, G., Barazangi, M., Al-Maleh, K., and Sawaf, T. (2001a), Tectonic and Geologic Evolution of Syria, GeoArabia *6(3)*, 573-616.

Brew, G., Lupa, J., Barazangi, M., Sawaf, T., Al-Imam, A., and Zaza, T. (2001b), Structure and Tectonic Development of Al-Ghab Basin and the Dead Sea Fault System, Syria, Journal of the Geological Society *158*, 665-674.

Cai, J.,McMechan, A., and Fisher,M.A., (1996), Application of ground penetrating radar for investigation of near surface fault properties in the San Francisco Bay rgion. Bull. Seis Soc.Am., 86, 1459-1470.

Caputo, R., Salviulo, L., Piscitelli, S., and Loperte, A., (2007), Late Quaternary activity along the Scorciabuoi fault ( Southern Italy) as inferred from electrical resistivity tomographies: Annals of Geophysics, Vol. 50, N. 2, P 213-224.

Caputo, R., Piscitelli, S., Oliveto, A., Rizzo, E., and Lapenna, V., (2003), The use of electrical resistivity tomographies in active tectonic: Examples from the Tyrnavos basin, Greece, Available online 5 June 2003, ArchEnviMat.

Chwatel, W., Decker, K., and Roch, K., (2005), Mapping of active capable faults by high-resolution geophysical methods: Examples from the central Vienna basin: Austrian Journal of Earth Sciences, Volume, 97.

Dobrin, M. (1976), Introduction to Geophysical Prospecting, Mc Graw-Hill, New York.

Demanet, D., Renardy, F., Vanneste, K., Jongmans, D., Camelbeeck, T., and Meghraoui, M., (2001), The use of geophysical prospecting for imaging active faults in the Roer Graben, Belgium: Geophysics, Vol. 66, No.1, P. 78-89.

Sabrina Y.F., Augusto E.R., Jose M. Cortes and Carla M., (2009), Characterization of Quaternary faults by electric resistivity tomography in the Andean Precordillera of Western Argentina, Journal of South American Earth Sciences, Vol 28, Issue 3, PP: 217-228.

Mares, S., ed., (1984), Introduction to Applied Geophysics, ( Reidel Publ Co., Dordrecht, Boston, Lancaster) P. 581.

Massoud, U., El Qady, G., Metwaly, M, and Santos, F. (2009), Delineation of shallow subsurface structure by azimuthal resistivity sounding and joint inversion of VES-TEM data: case study near Lake Qaroun, El Fayoum, Egypt, Pure Appl. Geophys. *166*, 701-719.

Orellana, E., and Mooney, H.M. (1966), Master Tables and Curves for Vertical Electrical Sounding Over Layered Structures, Interciencia, Madrid.

Palmer, J.R., Shoemaker, M., Hoffman, D., Anderson, N. L., Vaughn, J. D., and Harrison, R. W., (1997), Seismic evidence of quaternary faulting in the Benton hills area, southeast Missouri: Seis. Res. Lett., 68, 650-661.

Pichugin, N.I., and Habibullaev, I.K.H. (1985), Methodological Recomendations in Studying Geo-Tectonic Conditions of Vertical Electrical Soundings Data with Application of EC Computer for Solving Hydrogeological and Geo-Engineering Problems, Tashkend, (in Russian).

Parrales, R., Dahlin,T., and Rubi, C., (2003) , Site investigation with combined methods in a faulted area in Managua, Nicaragua- A pre-study: Procs. 9th Meeting of Environmental and Engineering Geophysics, Prague, Czech Republic, P-076.

Piscitelli, S., Caputo, R., Lapenna, V., Oliveto, A., and Rizzo, E., (2009), Electrical imaging survey across activity faults: Examples from the Tyrnavos basin, Greec, GNGTS-Atti del 21o Convegno Nazional/01.01

Ponikarov, V.P. (ed.) (1966), The Geological Map of Syria, scale 1:200000, sheets I-37-XIX and I-36-XXIV, Ministry of Industry, Damascus.

Shields, G., Allander, K., Brigham, R., Crosbie, R., Trimble, L., Sleeman, M., Tucker, R., Zhan, H., and Louie, J.N., (1998), Shallow geophysical survey across the Pahrump Valley fault zone. California- Nevada border: Bull. Seis Soc.Am., 88, 270-275.

Van Ardsal, R., Purser, J., Stephenson, W., and Odum, J., (1998), Faulting along the southern margin of Reeflot Lake, Tennese: Bull. Seis Soc.Am., 88, 131-139.

Williams, R., Luzietti, E, A., and Carver, D, L., (1995), High- resolution imaging of Quaternary faulting on the Crittenden County fault zone, New Madrid seismic zone, northeastern Arkansa: Seis. Res. Lett., 66, 42-57.

Zohdy, A.A.R. (1989), A New Method for the Automatic Interpretation of Schlumberger and Wenner Sounding Curves, Geophysics *54*, 245-253.

Zohdy, A.A.R., and Bisdorf, R.J. (1989), Schlumberger Sounding Data Processing and Interpretation Program, U. S. Geological Survey, Denver.
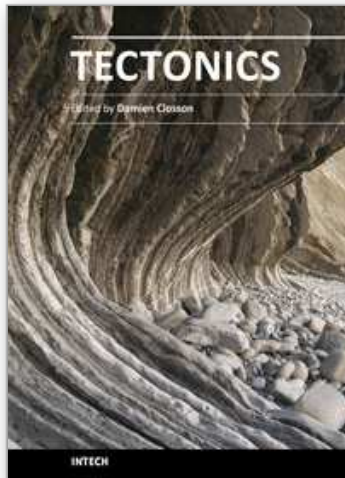
**Tectonics**

Edited by Dr. Damien Closson

The term tectonics refers to the study dealing with the forces and displacements that have operated to create structures within the lithosphere. The deformations affecting the Earth's crust are result of the release and the redistribution of energy from Earth's core. The concept of plate tectonics is the chief working principle. Tectonics has application to lunar and planetary studies, whether or not those bodies have active tectonic plate systems. Petroleum and mineral prospecting uses this branch of knowledge as guide. The present book is restricted to the structure and evolution of the terrestrial lithosphere with dominant emphasis on the continents. Thirteen original scientific contributions highlight most recent developments in seven relevant domains: Gondwana history, the tectonics of Europe and the Near East; the tectonics of Siberia; the tectonics of China and its neighbourhood; advanced concepts on plate tectonics are discussed in two articles; in the frame of neotectonics, two investigation techniques are examined; finally, the relation between tectonics and petroleum researches is illustrated in one chapter.

**How to reference**

In order to correctly reference this scholarly work, feel free to copy and paste the following:

Jamal Asfahani (2011). The Role of Geoelectrical DC Methods in Determining the Subsurface Tectonics Features. Case Studies from Syria, Tectonics, Dr. Damien Closson (Ed.), ISBN: 978-953-307-545-7, InTech, Available from: http://www.intechopen.com/books/tectonics/the-role-of-geoelectrical-dc-methods-in-determining-the-subsurface-tectonics-features-case-studies-f

# INTECH
open science | open minds